JPRS 78232

4 June 1981

China Report

SCIENCE AND TECHNOLOGY

No. 102

FBIS FOREIGN BROADCAST INFORMATION SERVICE

NOTE

JPRS publications contain information primarily from foreign newspapers, periodicals and books, but also from news agency transmissions and broadcasts. Materials from foreign-language sources are translated; those from English-language sources are transcribed or reprinted, with the original phrasing and other characteristics retained.

Headlines, editorial reports, and material enclosed in brackets [] are supplied by JPRS. Processing indicators such as [Text] or [Excerpt] in the first line of each item, or following the last line of a brief, indicate how the original information was processed. Where no processing indicator is given, the information was summarized or extracted.

Unfamiliar names rendered phonetically or transliterated are enclosed in parentheses. Words or names preceded by a question mark and enclosed in parentheses were not clear in the original but have been supplied as appropriate in context. Other unattributed parenthetical notes within the body of an item originate with the source. Times within items are as given by source.

The contents of this publication in no way represent the policies, views or attitudes of the U.S. Government.

PROCUREMENT OF PUBLICATIONS

JPRS publications may be ordered from the National Technical Information Service, Springfield, Virginia 22161. In ordering, it is recommended that the JPRS number, title, date and author, if applicable, of publication be cited.

Current JPRS publications are announced in Government Reports Announcements issued semi-monthly by the National Technical Information Service, and are listed in the Monthly Catalog of U.S. Government Publications issued by the Superintendent of Documents, U.S. Government Printing Office, Washington, D.C. 20402.

Indexes to this report (by keyword, author, personal names, title and series) are available from Bell & Howell, Old Mansfield Road, Wooster, Ohio 44691.

Correspondence pertaining to matters other than procurement may be addressed to Joint Publications Research Service, 1000 North Glebe Road, Arlington, Virginia 22201.

JPRS 78232

4 June 1981

CHINA REPORT

SCIENCE AND TECHNOLOGY

No. 102

CONTENTS

PEOPLES REPUBLIC OF CHINA

ABSTRACTS

CHEMISTRY

ENGINEERING

OBSERVATION OF A LASER-INDUCED HIGH EXPLOSIVE GROWTH PROCESS

Shanghai JIGUANG [LASER JOURNAL] in Chinese No 5-6, 1978 pp 163-164

[Text] This article introduces an experimental method in the observation of a laser-induced high explosive detonation growth process and the experimental results of using Tai-an (PETN) as a first powder charge.

The design principles of the testing set-up are twofold: (1) to facilitate the observation of the growth process of the laser-induced detonation. This requires a good hermeticity of the set-up and the laser's capacity to ignite easily the powder charge; (2) in order to directly observe the growth process of the detonation, conditions of good transparency of the set-up and a convenient method of installation are required. The function of the covering glass plate of the testing set-up is to prevent the splattering of the explosive when the powder charge surface is illuminated by a laser, and thus to prevent the cooling caused by the splashing of the dynamite. This preserves the initial temperature and pressure of the dynamite and is conducive to an accelerated reaction rate. The function of the fan-shaped slab of the plexiglas in the testing set-up is equivalent to an observation window; an air gap of 0.20 mm is established between the fan-shaped slab and the powder charge. When the explosive is ignited, the thin-layer of air will glow when compressed by a shock wave and a high speed camera will be used to record the process from ignition by laser to a normal detonation.

We are relying heavily on thermal effect in the discussion of the function of laser ignition of the explosive and the present experimental results can be approximately explained by a thermally induced explosion mechanism. According to the thermally induced explosion mechanism, because of the short interaction time of the laser, the powder charge can be treated as a semi-infinite space, neglecting the effects of convection, thermal radiation and radial conduction of heat. If parameters such as thermal capacitance, coefficient of thermoconductivity, and activation energy are taken as constants within the temperature range under study, and also the explosive surface is adiabatic, then an approximate one dimensional heat-flow equation can be used to describe the laser-induced explosion problem. The calculated results of the induction period is close to the measured experimental results.

Employing this testing set-up, several stages (induction--ignition--low speed detonation--high speed detonation) are observed in the laser-induced Tai-an (PETN) explosive process. If metallic powders are added in the explosive and appropriate

pressurized filling technique is selected, the time from ignition to detonation can be reduced to the order of 1 microsecond under a fixed energy environment.

The experimental results indicate that this kind of testing set-up is more suitable for detecting the development process of the tested detonation growth period from about 1 microsecond to 100 microseconds.

CSO 8111/1077

PROGRESS MADE IN STUDYING EFFECTS OF MICROWAVE BIOLOGY

Beijing SHENGLI KEXUE JINZHAN [PROGRESS IN PHYSIOLOGICAL SCIENCES] in Chinese No 4 Vol 11, 1980 pp 309-314, 360

[Article by Ye Guoqin [5509 0948 2953] of the Microwave Laboratory of the Zhejiang Medical University: "Progress in the Studies of the Effects of Microwave Biology"]

[Text] Microwave technology has wide applications in military science, communications, industry and medical sciences. Because microwave radiation can affect the health of human beings, many nations have established microwave safety codes to control its damage. In the 1970's, the study of the effects of microwave biology delved deeply into cellular and molecular levels. Some advanced technologies: electronic computer, electron microscope, electrophysiology of cells, holography have all been used by researchers. The central problem of the mechanism of the effects of microwave biology is the non-thermal effect. If this problem can be solved, some basic medical theories will be shaken.

Microwave technology is widely used in industrial heating and drying. It is widely used in guidance, aiming of artillery, and satellite telecommunications in military applications. It is used in the microwave accelerator of high energy particles and microwave spectrography in scientific research. When using microwave technology and if it is used improperly, or if necessary knowledge and measures of protection are lacking, it can be harmful to man's health. As early as the 1930's, the United States had begun to study the effects of microwave upon living organisms. In the 1950's, they had relatively thoroughly studied the electrical parameters of microwave effects in tissues of living organisms and proposed safety codes for using microwave. The Soviet Union and East European nations have proposed a safety code that is 1,000 times less stringent than that of the United States based on field surveys and physical checkups and have taken the non-thermal effect of microwave as the theoretical foundation.

In 1966, the International Microwave Power Institute (IMPI) was founded. The main members are the United States, Soviet Union, Great Britain, France and Canada. The headquarters is in Canada. There is the European branch (headquartered in London, New York) and the East European branch (headquartered in Warsaw, Ieper). The organ of the IMPI is the Journal of Microwave Power. After founding of the IMPI, an international academic disucssion conference on microwave has been held

annually. The most important conference was the Warsaw Conference (July, 1973). A total of 40 papers were presented, involving the effects of microwave upon the nervous system, the effects upon cells and molecules, combined effects of microwave and X-ray, the effects of microwave upon the reticuloendothelial system and the cerebral hypophysis. A total of 78 reports were presented at the Belgium Conference (1976).

Studies of the effects of microwave biology in the 1970's have already reached the cellular and molecular levels. Some advanced technologies, such as computer technology, electron microscopy, electrophysiology of cells, holography have all been used. But the mechanism of the effects of microwave biology: the serious opposition of the viewpoints of the thermal and non-thermal effects still remains.

The studies of the effects of microwave biology are described below according to the functional systems of the human body and the methods of study:

I. Thermal effect of Microwave

When microwave acts upon a living organism, only a portion of the energy is absorbed and converted to thermal energy. The microwave power absorbed by the tissues and the depth of penetration of microwaves are related to the dielectric constant, electrical conductivity, thickness and microwave frequency of each layer[1]. The shorter the wavelength, the less penetration into the tissue, the longer the wavelength and deeper the penetration. For example, the penetration of 2.5GHz is 9 mm. The penetration of 0.9GHz is 18 mm.

The thermal effect of microwave radiation is mainly manifested by a rise in the subcutaneous temperature and the quickening of breathing and heart beat. Faster breathing is the most obvious. The thermal effects of pulse wave and continuous wave are not visibly different. If the power of the microwave is too large, the amount of heat produced in the tissue will be greater than the ability of the tissue to disperse the heat, regulation of body temperature loses balance, finally causing death[2]. The threshold of microwave radiation to cause death is related to the intensity of radiation, the duration and the temperature and humidity of the environment[3]. According to widespread studies of the thermal effect of microwave conducted over the past 25 years, reversible or irreversible pathological changes can be produced by exposure to a power density of 100 mw/cm^2. In large animals, a power lower than 100 mw/cm^2 will not produce pathological changes or will only produce a very slight pathological change[4].

Because microwave can heat local tissues while the temperature of the rectum does not rise, we cannot eliminate the effect of localized heating upon the nerves and the sensory organs. We know from experimental results that the phenomena of a drop in electrical potential of the spinal cord caused by microwave and the drop in electrical potential caused by localized heating of the spinal cord are the same. At this time, using cold Ringl's solution to wash the spinal cord can bring the electrical potential back to its original level[5]. Temperature variations will affect the speed of conduction of nerve impulses and the speed of enzymic metabolism. Therefore microwave of a power density of 1 mw/cm^2 - 10 mw/cm^2 can produce a minute localized heating in the tissue. This should not be neglected. At

present, many European and American scholars have used the minute heating effect of microwave as the theoretical foundation to explain the pathological changes produced by microwave of less than 10 mw/cm^2. This is the last defense line to retain the theory of "thermal effects."

II. The Effect of Microwave Upon the Lens and the Visual Retina

In 1950, it was first reported that a radar technician who worked for one year with microwave of 1,500 - 3,000 MHz frequency and a power density of 100 mw/cm^2 developed cataracts on both sides[6]. From then on, the damage to the eyes by microwave has become a matter of concern. This has two meanings: 1. A low field intensity microwave will not cause cataracts. They used medication to dilate the pupil, used an eye examination scope to examine the bottom of the eye and the lens, and photographed and recorded the shape of the turbid vacuoles, their numbers and positions. The results showed there was no statistical difference between 736 microwave workers and the control group of similar age group. The so-called "microwave cataract" and ordinary cataract do not have extraordinary different form. 2. Microwave can hasten aging of the lens. There were visible differences between them and the control group. Out of 1,000 microwave workers, 42 were found to have cataracts. The lens of these people showed traces of heat damage. The damage was mostly on the posterior pole, and there were cases of recurring cataract. The microwave workers did not feel any sensation of sting or heating during the period of work. The cataract was discovered only after they went to the doctor because of reduced visual capabilities.

The research reports issued by the armed forces of the United States believed 10 mw/cm^2 would not damage the lens, 10 - 300 mw/cm^2 could cause reversible changes of edema of the lens, power larger than 300 mw/cm^2 could cause irreversible changes in the lens[7].

In experimental research, some people have designed a "dielectric lens." It can focus microwave energy to irradiate the eyes of animals. In this way, the animals can be far away from the antenna and the microwave energy received by the surface of the body of the animals can be neglected while the microwave energy focused in the lens can become sufficiently large[8]. Meafee designed a shadowgraph viewer and using it to examine cataracts provides many advantages[9].

Intense microwave irradiation can rapidly cause cataracts in animals. Cataracts can be caused in the eyes of rabbits in 5 minutes by irradiation of 60 mw/cm^2. The average temperature of the lens can reach as high as 55.1°C. Irradiation by 200 mw/cm^2 (30 minutes) each time or 100 - 200 mw/cm^2 for 30 minutes a day lasting a total of one month will not cause cataracts. But exposure of 15 minutes to 300 mw/cm^2 will produce vacuoles and turbidity in the lens. Some people have also reported that cataracts and vacuoles can be observed after exposure to 165 mw/cm^2 each day for 20 minutes each time, 20 times a day for a total of 36 times. The threshold value of the cataract in rabbits is 180 mw/cm^2 exposed for 140 minutes. The threshold value of monkeys is 300 mw/cm^2 exposed for 21 minutes. There are two types of experimental cataracts:

1. Cataract immediately occurs after exposure and it is accompanied by other damage to the visual structure (such as cornea, bloodshot iris). In the lens a sheaf-like turbidity appears and the lens fuses into an incomplete opaque body.

2. Several days or several weeks after exposure, the damage is localized in the back cortical substance of the lens. Repeated exposure can affect the entire lens.

Microwave cataract is mainly caused by the thermal effect of microwave. Because the function of heat dispersion of the lens is poorer, temperature easily rises, causing the protein in the lens to solidify and metabolism of the enzymic system is hindered. Weiter reported that microwave irradiation caused the vitamin C content in the lens to drop. Heating the lens will also bring the same result. Some also reported that exposure to 225 mw/cm^2 microwave irradiation will not cause changes in the metabolism of thymus pyrimidine nucleoside in the cornea cell. Turbidity of the lens is mainly due to changes of the structural arrangement of the body of the cells. Some people believe low intensity microwave's non-thermal effect will also cause cataracts. Some others oppose this opinion. There is no definite conclusion. Microwave irradiation will also cause pathological changes in the retina. Recently, it was discovered that low intensity microwave will interfere with the electrical potential of the retina[10].

III. Effect of Microwave Upon the Cardiovascular System

The effect of microwave upon the cardiovascular system comes mainly from Soviet reports[11, 12]. Workers under the effects of microwave for long periods have developed frequent weakening of the first sound of the pointed end of the heat and accompanied at the same time by noise during the systolic period. Persons exposed for long periods to intense microwave have developed symptoms of depressed heart sound and shifting of the heart's boundary. As early as 1948, there had already been reports of overly slow and overly rapid heart movement among microwave workers, especially those working around the centimeter wave segments. Soviet scholars believe this is a manifestation of disorder of the vegetative neurovascular function. About 36 percent of the microwave workers frequently have uneven heart beats. A few, about 2 percent, has early atrioventricular heart beat. Workers exposed to microwave for long periods show a lengthened atrioventricular conduction on the electrocardiogram. A few shows hindrance of atrioventricular conduction. The electrocardiograms may also show depression of the T wave and a drop in the ST segment and such phenomena of deficient blood supply in the coronary artery. Individuals may develop minute focal myocardial infarction.

Soviet scholars proved by 20 years of on-site surveys that the tenseness of the vagus nerve controlling the vegetative neuro-vascular reactions in workers working and exposed to long periods of several hundred w/cm^2 to several mw/cm^2 intensities of microwave has increased and blood pressure has dropped. They constitute 22.6 to 28 percent. Their systolic pressure can be lower than 100 mmHg. The proportion of females is higher. The urine of one day and night of a microwave operator may contain as high as 42 to 52μg% of excreted adrenaline (the normal value is 26 to 40μg%) and pure adrenaline of 65 to 80μg% (the normal value is 58 to 68μg%). Clinical symptoms of an increase in the secretion of catechu phenol ammonia and deficient blood supply to the heart exist simultaneously. It can be inferred from this that microwave causes disorders of the function of the sympathetic nerve-adrenal system and the lower part of the thalamus[13].

Some subjected dogs to 5 mw/cm^2 microwave irradiation. After only 30 minutes, changes in the electrocardiogram occurred. The QRS interval extended and the heart

beat slowed. Normalcy returned 1 hour after exposure. Exposing the heart removed from the frog to microwave of a power density of several tens mw/cm^2 will stop the heart beat. The use of an average power of 30μw/cm^2 of microwave to irradiate the heart for 10 s 200 ms after the P wave will interfere with normal heart beat. The above phenomenon will not occur when the heart is exposed to 10μs 0 - 100 ms after the P wave[14]. But, the results of this experiment cannot be repeated. R. M. Clapman and G. A. Cain[15] used 200 hearts removed from the body of frogs and exposed them to pulse microwave and ECG synchronous stimulation and then used the computer to process the changes in heart beat. Visible statistical differences in the heart beat of the stimulated group and the control were not discovered. Frey repeated past experiments and still firmly believes the view that microwave interferes with normal heart beat.

Whether low field intensity microwave causes any damaging effect upon the cardiovascular system is still being debated and further research is required.

IV. The Effect of Microwave Upon Blood, the Endocrine and Sexual Functions

Microwave does not greatly affect red blood cells. Changes in white blood cells vary with different wavelengths. Centimeter wave causes them to increase, millimeter wave causes them to decrease. Reticular cells and platelets generally decrease and lymphocytes increase. A decrease in the functions of the blood making system and the lymphatic system occurs 6 weeks after exposure to 0.5 mw/cm^2 microwave for 2 hours each day. Ordinarily, normalcy returns 2 months after exposure has ceased. Some have injected staphylococcus into the veins of the domesticated rabbit to infect it and then exposed the rabbit to microwave. The white blood cell count and the granulocyte count were taken 4, 6, 10 and 14 days before and after infection. The counts of the group exposed to microwave all dropped. Some believed the reaction of peripheral blood to microwave irradiation was not the result of the thermal effect of such exposure but was the result of nervous reflect. However, the experimental results are still divided. Some used 10 mw/cm^2 microwave to irradiate animals each day for 2 to 3 hours lasting 6 months. The counts of white blood cells, hemoglobin and platelets in animals did not visibly drop. When animals were exposed to microwave irradiation during the early period of recovery from X-ray irradiation, the formation of white blood cells and red blood cells was stimulated and the condition of the marrow improved[16]. Therefore they proposed that microwave seemed to be able to serve as supplementary treatment of radiation diseases.

The total protein and globulin in the serum exposed to microwave irradiation for long periods rose while the ratio of albumin and globulin dropped. In most people, the content of chloesterin increased (260 - 410 mg percent), the content of chlorides in blood dropped, the secretion of sodium chloride in urine increased, the content of histamine in blood was higher than normal by 1.5 to 2 times. The activity of alkaline phosphorylase in the white blood cells visibly increased. Low intensity microwave increased the content of free amino acids in blood, high intensity microwave irradiation reduced their content. Intense irradiation will cause visible changes in iron, copper, cobalt, zinc, calcium and megnesium ions and proteins containing metallic elements in the blood and the tissues and organs. Exposure to less than 10 mw/cm^2 will not cause any change. Microwave can also

cause the content of mercapto-radicals in the blood to drop. This drop coincides with the symptoms of the patient subjected to microwave irradiation. Therefore it is believed measurement of the content of mercapto-radicals in the blood can serve as an indicator for early diagnosis of microwave damage. Low intensity microwave does not visibly affect platelets and the time of clotting of blood. But high intensity (280 mw/cm^2) will cause a delay in the clotting time and shorten the time of contraction of clots.

In immunobiology, microwave irradiation suppressed the formation of antibodies and even caused globulin antibodies to disappear completely[17]. Microwave also increased the serum complement of the body and reduced the content of immunal globulin[18].

These all show microwave visibly affects the ability of immunity of the body.

The effects of microwave upon the endocrine have already become an important concern[19]. Microwave of small intensity (< 10 mw/cm^2) will cause disorder of the function of the thalamus-pituitary-adrenaline functions and increase the activity of CRF, ACTH[20]. Microwave can also cause hyperfunction of the thyroid gland in a few patients, cyanosis of the hands and feet, reduced function of mammary secretion in women, endocrine disorder of the metabolism of sugar, causing visible drop in blood sugar and blood phosphorus. Experimental research has pointed out [21,22] that 1.5 - 3.3 mw/cm^2 of microwave irradiation caused the content of serum pentacarboxylic acid in the small white mice to increase. The same changes were not seen when the mice were subjected to infrared irradiation of the same field intensity. Also, a frequency of 2.4 GHz caused an effect but frequencies of 2.9, 5.4, 9.4 GHz of microwave of the same intensity did not produce any effects. Microwave can suppress secretion of thyroxin. Microwave irradiation does not affect serum proteinase[23], the radiation effect of Ga^{++} upon the mitochondria of the liver of the white mice[24,25], and the glucose-6-phosphate dehydrogenase. Some believed the effect of microwave upon enzymes is the thermal effect and it does not exert any special effect on enzymes[26]. No increases [27] were observed in the 17-OHCS and 17-KS measured in urine.

There have already been reports of microwave affecting sexual functions[28]. A 31-year-old man was repeatedly subjected to high power radiation from radar for over 4 years. Pathological anatomy of the testicles showed localized focal nercosis of the seminal curvature duct, atrophy and mesenchyme edema. The production of sperm reduced. One year after exposure ceased, his sexual function began to recover. Some people believe that a 5 mw/cm^2 field intensity can damage the testicles[29], causing the temperature of the testicles to rise to 37°C[30], because local body temperature here rises easily. Some people are exploring male sterilization by microwave based on this principle. Experimental research shows microwave can reduce the ability of the hen to lay eggs. The effect of microwave upon sexual functions are manifested clincally by impotence of the male and disorder of the menstrual cycle of the female.

Microwave irradiation of pregnant white mice can cause the fetus to die[31] and suppress growth and development of the individual[32], but there are also completely opposing opinions.

V. Effect of Microwave Upon the Central Nervous System

Study of the effects of microwave upon the central nervous system has already been given special attention[33]. Survey of microwave workers shows the hindrance of the functions of the central nervous system is manifested by headaches and dizziness, physical weakness, tiring easily, irregular sleep (sleepiness during the day and a lot of dreams at night), failing memory, and excitability. The proportion of patients suffering from dizziness, weakness, insomnia, amnesia is the highest[34,35]. Electroencephalographic examinations show an increase of slow waves. Some believe the occurrence of slow waves is a manifestation of the suppression process of the nervous system. This is because experiments prove that the excited phase of animals after being given harbital anesthesia is reduced by exposure to microwave irradiation[36]. Some people exposed white mice to microwave of 5 ± 1 mw/cm^2 in intensity and observations of the electroencephalograms taken 1 - 7 days and 1 and 5 months afterwards showed microwave can cause changes in the electroencephalograms[37]. Also, it was discovered that the content of cholinesterase and isotope P^{32} in the brain dropped[38]. Some people believe the effects of microwave upon the electroencephalogram are not chronic cumulative effects. Microwave can even induce epileptic breakouts in the encephalograms of animals. Visible waves appear in the spontaneous electrical potential. Normalcy returned 48 to 72 hours after exposure ceased. Some people conjecture that this might have been caused by the excitation of the upward excitation system of the reticular system and interception and hindrance of the downward suppression system by microwave. But the effects of microwave still remained after severing the cerebral tissue at the mesencephalon level. Slow waves occurred widely in the cortex but the effect on the occipitalis is the most visible. Opinions on the threshold strength of microwave in affecting the electroencephalogram are diverse. Some people even believe slow waves can be produced by an intensity of 10 - 250$\mu w/cm^2$ [39]. The intensity that determines the activeness of microwave biology is 5 - 20$\mu w/cm^2$. Viewing the changes of the biochemical indicators of the brain and the changes of the electroencephalogram, pulse wave is more active than continuous wave.

In research technology, the "microwave filter" (also called low passage wave filter) has been used, enabling the operator to observe and record the electroencephalogram during exposure to microwave irradiation without being exposed to microwave. Some have also used the method of regulating the brain wave frequency to avoid interference from microwave to observe the changes in the brain's electrical potential.

The activity of the glandular purine radical and tryptophane in the brain is increased in animals exposed to 10 mw/cm^2 of irradiation. The substance of contracted blood vessels of the inferior thalamus and the thalamus increased slightly while the activity of monoamine oxydase did not show any change If the field intensity is greater than 20 mw/cm^2, vacuoles can appear at the inferior thalamus and the base thalamus. Intersections of the visual nerves had degenerate fibers. The thalamus, the exterior patelliform, the Purkinje cells did not show any change. But there are also some people who believe exposure of long periods to low field intensity microwave will cause changes in the form of brain tissues and tissue chemistry (chromatocyte oxydase, succinic acid dehydrogenase, acetyl cholinesterase), and at the same time, metabolic disorders of the marrow phospho-ester and neuroglia also occur. Irregular chromatic spherules were found in the cerebellum

and cerebral white and neuroglia cells increased. The amounts of cholinesterase and acetyl choline both changed. Microwave irradiation caused some enzymes in the brain to lose their activity, for example, the activity of the myokinase was only 10 percent that of the control. The phosphokinase in the brain was not affected, therefore the glucose phosphorylation process was still normal.

Using conditioned reflex and Y maze experiments showed animals became slow in their motion after being exposed to microwave irradiation. They even did not respond to food. The incubation period of conditioned reflex was longer, and the ability to memorize decreased. At this time, slow waves occurred in the electroencephalogram of the cortex and the hippocampal circle showed convulsive electrical discharge. These gradually disappeared after exposure ceased. Microwave does not have much effect on the induced electrical potential in the cortex.

Study of the effects of microwave upon the behavior of animals has caught people's attention[40]. An exposure of 1 mw/cm for 185 hours does not affect spontaneous movement of animals[41]. After being exposed to 6 mw/cm^2 the exploratory behavior of animals lessened, and guarding recognition behavior of animals was affected while swimming was not affected[42]. The ability of repeated taking was more easily affected by microwave than its recognizing ability. Microwave affects the offensive behavior of animals[46]. Pulse wave has a greater effect on the activeness of behavior than continuous wave[43,44]. Suppression of behavior, slow waves of the encephalogram and increased release of $^{45}Ga^{++}$ in the brain often occur simultaneously[45].

The effects of microwave to induce heating of the skin and pain are determined by the intensity and duration of exposure and the area exposed. When a 40 centimeter^2 area of the face is exposed to microwave of 21 mw/cm^2 (10 GHz) or 58.6 mw/cm^2 (3GHz), warmth can be felt after 1 second. When the power density is lowered by half, the threshold of warmth is 4 seconds. If the entire face is exposed to microwave with a power of 4 - 6 mw/cm^2 (10 GHz), warmth can be felt in 5 minutes. When the power is 10 mw/cm^2, it only requires 0.5 seconds. Pain can be felt in 3 minutes when an area of 9.5 centimeters^2 of the inside upper arm is exposed to microwave (3 GHz) with a power of 830 mw/cm^2. When the power is 3.1 w/cm^2, pain is felt in 20 seconds. The threshold of pain of large area exposure (53 centimeters^2) is 560 mw/cm^2. The heating of the skin and the threshold of pain can be used as the subjective sensory indicators of the individual to protect himself from sudden intense irradiation. Working and being exposed to microwave for long periods can raise the threshold of pain.

Microwave workers with a longer work history have less sensitive smell and vision. The non-thermal power ($<$ 10 mw/cm^2) will reduce the hearing sensitivity of animals after a long period of stimulation. The incubation period of reactions is extended. The electrical activity of the organ of Corti of the cochlea of the guinea pig exposed for 4 hours each day for 25 to 50 days to 10-centimeter microwave of a power of 2 mw/cm^2 was weakened. The activity of the lactadehydrogenase in the organ of Corti increased, while the activity of succinic acid dehydrogenase of the acetyl cholinesterase was reduced. When exposed to 918 MHz microwave irradiation, the wave forms of 50 KHz and 50 v could be recorded on the cochlear window of the guinea pig, afterwards, the electrical potential of the hearing potential was

recorded. Electrical activity can also be recorded on the cerebral temporal lobe. After the animal has died, these responses disappear. Therefore it is believed microwave can cause a microphonic effect in the cochlea[47]. The microwave hearing threshold of the human being is 120μw/cm (2450 MHz, background noise 45 decibel). The microwave hearing threshold of the cat is 178μw/cm (2450 MHz, background noise 64 decibel). Some people believe microwave hearing reaction is a new research tool to study man's hearing reaction and mechanism. Microwave can also stimulate the vestibule. This stimulation may be related to the production of heat by microwave. For example, when a monkey is exposed to 10 mw/cm^2, 600μcal,/g,sec of heat can be produced in the brain. Recently, Guy and Chou[48,49] of the United States have proposed the theory of "thermoelasticity" to explain the hearing effect of microwave.

VI. Study of the Effect of Microwave Upon the Function of the Single Cell

In recent years, much research has been done to study the effects of microwave upon the growth of cells, synthesis of RNA, DNA, and synthesis of enzymes. Many people have reported that microwave irradiation can increase the permeability of the cell membrane, cause disorder of the function of cellular and subcellular structures, including suppression of the growth of cells and damage of the mitochondria. When the cell of the Chinese mouse (in a culture) was exposed to nonthermal intensity of microwave irradiation, it was discovered that its growth rate slowed by 10 to 60 percent. More quantities of magelophyknotic cells appeared and the changes were irreversible. After the embryonic cell of a chicken was exposed to 2.7 GHz, 0.5 mw/cm^2 or microwave irradiation, a protuberance occurred after 24 hours, and then it broke up and decomposed. The effect of irradiation of 1 mw/cm of microwave upon the granuloleucocyte suspended mixture was not large but at 5 mw/cm^2 the death rate of cells increased. The Reith (?) spectral analysis shows the amounts of energy of the various frequencies of the microwave absorbed by the tumor cell and a normal cell are different. The absorption of the energy of the microwave of frequencies of 50 - 200 GHz by the tumor cell varies according to the type of the cell. Ordinarily, there are two to four different frequency bands. There is a constant frequency difference between frequency bands. This may be due to the different material metabolism of the normal cell and the tumor cell. Because of this observation, the various ideas and exploratory attempts to use microwave in the early diagnosis and treatment of tumors have emerged.

Other experimental results show that microwave cannot suppress the growth and propagation of bacteria. It is ineffective even when the field intensity has reached 50 mw/cm^2, or even to stimulate growth and propagation. Some have also reported that the DNA structure of bacteria cannot be damaged by exposure to 60 mw/cm^2 for 30 minutes. Exposure of a cell (absorption power of 14 mw/g) of the embryo of the quail egg to 30 mw/cm^2 did not induce any visible change in the weight, red blood cells and white blood cells.

Wachtel et al used microelectrode techniques to study the electrical discharge characteristics of the cells of the nervous regions irradiated by microwave. They showed microwave causes the resting electrical potential to drop. The author believes this was caused by the change in the nature of the cell membrane, not a result of the heating effect of microwave[50]. Recently, Wachtel, H. proposed

the theory of over polarization of cells caused by microwave[51], and believed the non-thermal effect actually exists[52]. Thus, some proposed the theory of the effects of electromagnetic field and biological membrane. This theory holds that the pieces of phospho-ester of the protoplasmic membrane in the gaps between the brain tissues form the electromagnetic field that acts upon the central nervous system and serve as the material base.

The central problem of the mechanism of the effect of microwave biology is the non-thermal effect. Reviewing the information published previously, most people believe this effect exists. But, to convincingly argue its existence is still the main direction of study in microwave biology for the next few years. Its significance will far surpass the scope of protection against microwave. It will shake the basic theories of medical science.

REFERENCE

1. Schwan HP: "IEEE Transactions on Microwave Theory and Techniques," MTTT-19:146, 1971

2. Ye Guoqin [5509 0948 2953], Jiang Kui [1203 2849]: SHENGLI XUEBAO (JOURNAL OF PHYSIOLOGY) 32(1): 10, 1980

3. Mills WA: J Microw Pow 6:141, 1971

4. Michaelson SM: "Biologic Effects and Health Hazards of Microwave Radiation," Polish Medical Pub., p 1, 1973

5. Taylor EM, Ashleman BT: Ann NY Acad Sci 247:63, 1975

6. Hirsh FG, et al: Arch Indust Hyg Occup Med 6:512, 1952

7. Michaelson SM: "IEEE Transactions on Microwave Theory and Techniques," MTT-19:131, 1971

8. Carpenter BL, et al: Ann NY Acad Sci 247:142, 1975

9. McAfee RD, et al: Ann NY Acad Sci 247:135, 1975

10. Ye Guoqin [5509 0948 2953], Jiang Kui [1203 2849]: SHENGLI XUEBAO 32, 1980

11. Sadchnkova MN: Hygiene Works (9):10, 1971

12. Glottova KV: Hygiene Works (7):24, 1970

13. Burdenko T.M: Hygiene Works (10):49, 1973

14. Franklin P: J Microw 8(9):14, 1969

15. Clapman R.M, Cain C.A.: J Microw Pow 10(4):411, 1975

16. Rotkovska D, Vacek A: J Microw Pow 11(2):141, 1976

17. Dronov I.S: Hygiene Works (9):15, 1972

18. Servantie B, et al: J Microw Pow 6:59, 1971

19. Michaelson SM, et al: Ann NY Acad Sci 247:21, 1975

20. Muramov B. F., Krasnobaev L.E.: Military Medical Journal (1):56, 1975

21. Deficis A, et al: J Microw Pow 11(2)137, 1976

22. Parker LN: Am J Physiol 224(6): 1388, 1973

23. Allis JW: Ann NY Acad Sci 247:312, 1975

24. Elder JA, Ali JS: Ann NY Acad Sci 247:251, 1975

25. Strautb KD, Carver P: Ann NY Acad Sci 247:292, 1975

26. Yeargers EK, et al: Ann NY Acad Sci 247:301, 1974

27. Szady J, et al: J Microw Pow 11(2)139, 1976

28. Rosenthal DS, et al: J Am Med Assoc 205:245, 1968

29. Soad Ted: J Microw 12:20, 1969

30. Mchees BD, Finch ED: Adv in Biol Med Phys 14:164, 1973

31. Dietzel F: Ann NY Acad Sci 247:367, 1975

32. McAfee RD, et al: J Microw Pow 8:111, 1973

33. Leader: J Microw Pow 10(2): 127, 1975

34. Sadcikova MN: "Biologic Effects and Health Hazards of Microwave Radiation," Polish Medical Pub. p 261, 1973

35. Drogichina E.A: Hygiene Works (3):28, 1962

36. Goldstein L, Sisko Z: "Biologic Effects and Health Hazards of Microwave Radiation," Polish Medical Pub. p 128, 1973

37. Bertharison G: J Microw Pow 6:62, 1971

38. Baranski S, Edelwehn Z: Ann NY Acad Sci 247:109, 1975

39. Asabaev: Weekly Bulletin of Experimental Biology (7):56, 1972

40. Justesen DR: Ann NY Acad Sci 247:408, 1975

41. Roberti B, et al: Ann NY Acad Sci 247:417, 1975

42. Hunt EL: Ann NY Acad Sci 247:440, 1975

43. Thomas TR: Ann NY Acad Sci 247:425, 1975

44. Frey AH, et al: Ann NY Acad Sci 247:433, 1975

45. Bawin SM: Ann NY Acad Sci 247:74, 1975

46. Frey AH: Unpublished

47. Chung-Kwang Chou: J Microw Pow 10(4):361, 1975

48. Chung-Kwang Chou, Guy AW: Unpublished

49. Chung-Kwang Chou, Guy AW: Unpublished

50. Wachtel H, et al: Ann NY Acad Sci 247:46, 1975

51. Beaman RL, Wachtel, H: J Microw Pow 13(1), 1978

52. Wachtel H: Unpublished

9296
CSO: 4008/281-B

EFFECT OF AXIAL FORCES ON SHEAR STRENGTH OF REINFORCED CONCRETE STRUCTURAL COMPONENTS

Nanjing NANJING GONGXUEYUAN XUEBAO [NANJING INSTITUTE OF TECHNOLOGY] in Chinese No 4, Dec 79 pp 25-35

[Article by Lu Zhitao [0712 1807 3447], Zhou Minghua [0719 2494 5478] and Di Zhixin [3695 1807 2450]: "Effect of Axial Forces Upon the Shear Strength of Reinforced Concrete Structural Components Subjected to Bending"*]

[Text] Abstract

This article describes the experimental results of a total of 43 reinforced concrete structural components subjected to a combination of shear force, bending moment and axial force. It studies the causes, the main parameters and the degree of intensity of the effects of axial pressure and pull upon the shear strength of reinforced concrete structural components subjected to bending. It also discusses several related problems. Finally, it suggests a method of calculation based on the experimental results.

In actual construction, many reinforced concrete structural components are subjected to a combination of shear forces, bending moment and axial forces, for example, the upper chord and the lower chord of the frame of an empty house, the wall of a rectangular swimming pool, the wall and the floor boards of an underground drainage ditch. Especially under seismic forces, pillars of multistoried buildings bear large shear forces, bending moment and axial forces (pressure). On some pillars (such as angular pillars), pull can be generated by seismic load, making the pressured pillar become a pulled rod. On top of this, there are also shear forces and bending moments. Under the action of seismic forces, the double columns of single story houses and factory buildings also become structural components subjected to pulling (and pressure), bending and shear forces. In addition, because contraction is confined or because of temperature changes and changes in dimension, axial pulling forces can also be produced in the horizontal beams. But, the question of the shear strength of the structural component subjected to axial forces, shear forces and bending moments simultaneously is not yet reflected and solved in our nation's design codes (TJ10-74).

---

*This article was received on 12 October 1979.

For this, we have joined our efforts with the problem of the design of the shear strength of the vertical wall and the floor board (as shown in Figure 1) of the box shaped drainage ditch at the Mouwei Mines of the Maanshan Steel Mill and conducted preliminary experimental studies of the effects of axial pressure upon the shear strength of structural components subjected to bending. Then, we supplemented a batch of experiments on the effects of axial pulling forces, and explored the method of calculating the shear strength of the oblique section of the structural component subjected to eccentric forces (pressure or pull).

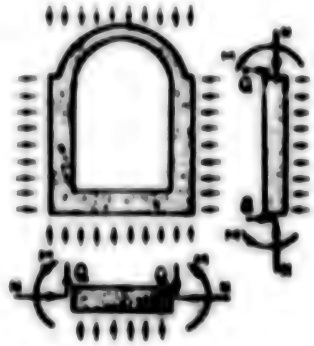

Figure 1.

I. Research Plan and Process of the Experiment

We experimented with and studied a total of 43 structural components. The first batch had 28 structural components. We mainly studied the effect of axial pressure upon shear strength. The second batch had 15 structural components. Emphasis was on the study of the effect of axial pull upon shear strength. The major parameters of the experiment and study were:

1. Axial force and direction: from the pulling stress $\frac{N}{bh} = -33.5$ kg/cm^2 to a pressure stress of $\frac{N}{bh} = 55.5$ kg/cm^2;

2. Hoop fitting percentage is 0, 0.28 percent and 0.32 percent;

3. Resistance of concrete to pressure: 122-319 kg/cm (original design was No 200 and No 300);

4. Longitudinal hoop fitting percentage is 2.69 percent, 2.04 percent and 2.46 percent;

5. Shear-span ratio is 2.5, 1.7 and 2.35.

In addition, among the two batches of beams, there were five beams that changed the position of longitudinal forces.

The purpose of selecting the above parameters was to enable us to study the effect of axial force upon the shear strength of the structural components within a relatively broad range and to explore the problem of the computational expression for the shear strength of the reinforced concrete beam under the effect of axial force.

1. Experimental structural components--All test components were reinforced concrete rectangular section beams. To make sure that they break, more longitudinal pulled steel reinforcements and an appropriate amount of longitudinal pressured steel reinforcements were fitted inside the beam. The longitudinal steel reinforcements were of II grade steel, the hoop reinforcements were No 3 steel. The test components were manufactured respectively by the Maanshan 17 Metallurgical Construction Company No 1 and the Nanjing Structural Components Plant. When manufacturing each batch of structural components, concrete test pieces of 10 x 10 x 10 cm were simultaneously made and were placed beside the structural components for maintenance. The experimental parameters and characteristics of each beam are detailed in Tables 1a and 1b.

Table 1a. Characteristics of Eccentric Pressure Shear and Eccentric Pulling Shear of the First Batch of Test Components

Group	Number	Dimensions of the section $b \times h_0$ (cm)	Strength of concrete R (kg/cm^2)	A_s/A_s' (cm^2)	Hoop reinforcement: Amount	Hoop reinforcement: Yielding point	Shear-span ratio a/h_0	Axial force N (ton)	Remark
I	N-1	15.3×32.2	246	3.08/12.90	φ6 @150	3420	2.5	0	
	N-2	15.0×32.1						7.5	
	N-3	15.3×31.9						15.0	
	N-4	15.2×31.8						22.5	
II	N-5	15.4×31.6	187	3.08/12.90	0		2.5	0	
	N-6	15.1×32.0						7.5	
	N-7	15.2×31.8						15.0	
	N-8	15.1×31.5						22.5	
III	N-9	15.2×31.5	236	3.08/9.82	0		1.7	−10.0	
	N-10	15.3×31.9			φ6@150	3420		−10.0	
IV	N-11	15.2×31.8	164	3.08/9.82	φ6 @150	3420	1.7	0	
	N-12	15.2×32.1						7.5	
	N-13	15.1×32.1						15.0	
	N-14	15.1×31.3						22.5	
	N-15	15.2×32.2						30.0	
V	N-16	15.2×32.0	136	3.08/9.82	0		1.7	0	
	N-17	15.3×32.2	185					7.5	
	N-18	16.0×32.4	185					0	
	N-19	15.6×32.6	185					22.5	
	N-20	16.0×31.6	185					30.0	
VI	N-21	15.0×31.8	315	3.08/9.82	φ6 @150	3420	1.7	20.0	$e = +6.8$ cm
	N-22	15.7×32.0						20.0	$e_0 = -6$ cm
	N-23	15.5×31.6						20.0	
	N-24	15.8×31.8						0	
VII	N-25	15.2×31.4	304	3.08/9.82	0		1.7	0	
	N-26	15.0×30.4						10.0	
	N-27	15.3×32.1						20.0	
	N-28	15.3×30.9						30.0	

Table 1b. Characteristics of Eccentric Pressure Shear and Eccentric Pulling Shear of the Second Batch of Test Components

Group	Number	Dimensions of the section bxh_0 (cm)	Strength of Concrete R (kg/cm²)	$\frac{A_s}{A_g}$ (cm²)	Hoop reinforcement: Amount	Hoop reinforcement: Yielding point	Shear-span ratio a/h_0	Axial force N (ton)	Remark
1	1	14.2×28.7	266	2.26 / 9.28	φ6 @150	3145	2.35	0	
	2	14.3×29.4						−7.5	
	3	14.0×29.1						−13.8	
	4	13.8×28.6						−14.8	
2	5	14.1×29.0	285	2.26 / 9.82	φ6 @150	3145	2.35	0	
	6	14.1×29.5						−10.0	
	7	14.2×29.0						−15.0	
3	8	14.3×29.1	197	2.26 / 9.82	φ6 @150	3145	2.35	0	
	9	14.5×29.4						−11.0	
	10	14.4×29.0						−15.0	
	11	13.9×29.2						+15.0	
	12	14.7×28.4						+15.0	e_0 = +9.5cm*
4	13	14.1×29.2	214	2.26 / 9.82	φ6 @150	3145	2.35	+15.0	e_0 = −9.5cm
	14	14.3×28.8	192					+15.0	
	15	14.0×28.8	122					+15.0	e_0 = +9.0cm

* The three structural components, 12, 13 and 15 with different values of e_0 are not subjected to a longitudinal force at the axial core. The force is eccentric. e_0 is positive means the longitudinal force acts on the pulled side, when it is negative, it means the longitudinal force acts on the pressured side.

The structural components subjected to axial pull were encased in steel tubes of an inner diameter of 5 cm beforehand at the time of manufacture. To measure the stress of the hoop reinforcements and the longitudinal reinforcements, small pieces of wood (5 x 3 cm) were tied to some of the hoop reinforcements and longitudinal reinforcements inside the beam before pouring the concrete to provide space for placing electrical resistance plates. The outer dimensions and the positions of the measuring points and the hoop fittings of the experimental structural components are shown in Figure 2.

2. The experiment--The axial pressure (pressure is applied at the center of the outer dimensions of the structural component) is applied to the surfaces of the ends of the beams by pulling rods and horizontal beams, jacks and ball reamers on the two sides of the beam. To eliminate adverse effects caused by the uneven surface of the ends of the beams, a layer of cement mortar of high strength was applied between the ball reamer and the surface of the end of the beam. The horizontal force is applied by the jack on the top surface at the center of the beam. A steel cushion of 2 cm thick and 15 x 5 cm in dimension was also placed between the surface of the top of the beam and the jack. Beneath the steel cushion was a thin layer of sand.

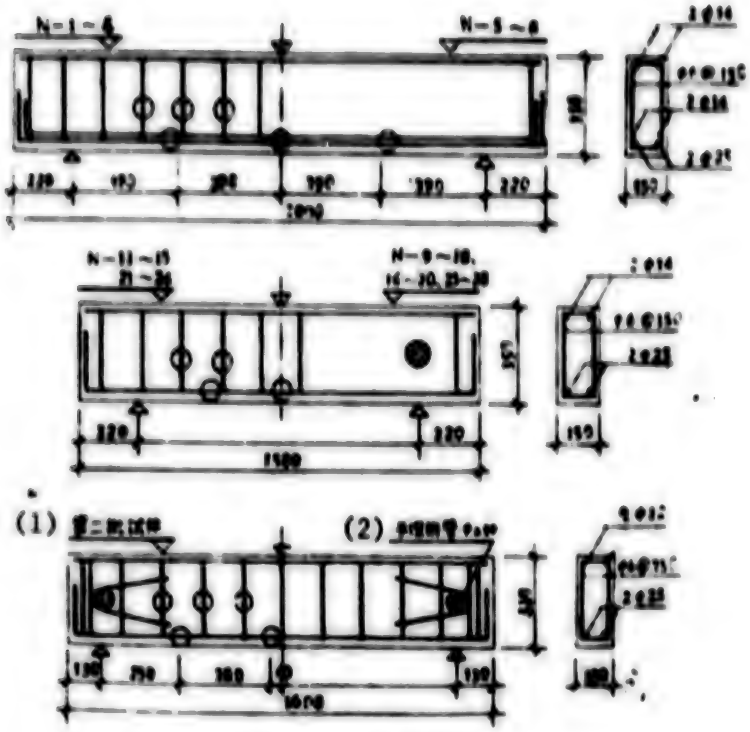

Figure 2

Key: (1) Second batch of test components
(2) Preset steel tube

The axial pull is also applied by the horizontal jack. It applies pressure to the experimental structural components via the steel pin (placed in the beam beforehand) inside the steel tube and the steel pulling rods on the two sides of the beam and the rectangular steel frame. Horizontal force is also applied by the jack on top of the beam.

To understand the effect of the applied horizontal force on the recoiling force of the support, when applying the horizontal force, the recoiling force of the support was also measured using sensors and electronic scales.

3. Contents of measurements and instruments--

Strain of shear-span on the inner section--25 cm calibrated hand-held extensometer (1/1000 readings);

Strain of the mid span section--hand-held extensometer and 4 cm calibrated electrical resistance plates;

Strain of the hoop reinforcements and longitudinal reinforcements--1.5 cm electrical resistance plates;

Strain of fibers of the pressured concrete rim--4 cm calibrated electrical resistance plate;

Deflection--1/100 reading;

Occurrence and expansion of cracks--40 magnification magnifying glasses for reading.

All the above electrical assistance measuring points are connected to the automatic recording YJS-8 strain meter.

4. Process of the experiment--Regardless of whether it is a pressure shear experiment or a pulling shear experiment, in all cases, axial force was first applied.* Generally it was applied two times (each time half of the axial force was applied). After applying each axial force, the readings of the meters were read. For the pulling shear structural components, after applying the axial force, cracks were observed and drawn. Then, horizontal loads were gradually applied and new cracks appeared and were observed on the surface of the structural components. The readings of the instruments were read. At the same time, attention was paid to keeping the axial force constant. The forces were continually applied until the experimental structural components broke.

II. Results and Analysis of the Experiments

1. General Situation of the Cracking and Breaking Process

The results of the experiments of all 43 experimental structural components are found in Tables 2a and 2b.

As references (1) and (2) pointed out, the resistance to cracking and shear strength of the oblique section of the reinforced concrete structural components increased because of the existence of the axial pressure. Conversely, they weakened because of the action of the axial pulling force.

Under the action of horizontal force, perpendicular cracks first appeared in the mid span. Then as the load increases, slanted cracks due to bending and shear forces emerged one after the other. The first cracks were perpendicular, then the cracks slanted towards the point of loading. When the load increased, slanted cracks due to belly shear forces emerged near the axis and in the section at a definite distance from the loading point. When the load increased further, new slanted cracks continued to occur and the original cracks extended and widened.

On the beam under the action of axial pressure, perpendicular cracks and slanted cracks emerged relatively late. Their speed of extension and widening was slower than that on beams subjected to nonaxial pressure and axial pull. Also, within a large area near the support, there were no cracks, therefore, these beams seemed to be stronger.

---

* According to reference (7), the order of applying axial force and horizontal loads does not greatly affect the limiting load bearing ability of the beam.

Table 2a. Experimental Results of the Eccentric Pressure Shear and Eccentric Pulling Shear of the First Batch of Test Components

Number	$\frac{N}{R_a bh}$	Experimental results M_j^s (T.M)	Q_j^s (T)	Q_u^s (T)	Form of breaking	Calculated according to the normal method Q_p'	Q_p'/Q_u^s	Calculated according to the suggested method Q_p''	Q_p''/Q_u^s
N-1	0	3.03	5.63	12.15	Shear pressure	13.50	1.11	13.50	1.11
N-2	0.081	2.93	6.87	14.38		13.37	0.93	13.83	0.96
N-3	0.162	3.90	8.75	15.62		13.39	0.86	14.32	0.91
N-4	0.243	4.37	9.38	15.31		13.31	0.87	14.69	0.96
N-5	0	2.93	5.00	6.58	Shear pressure	3.92	0.60	5.44	0.83
N-6	0.106	3.42	6.25	8.75		3.89	0.45	5.86	0.67
N-7	0.212	3.42	7.50	8.75	Splitting	3.89	0.46	6.33	0.72
N-8	0.318	4.39	8.75	11.10	Shear pressure	3.83	0.35	6.75	0.61
N-9	1.16*	1.35	5.00	9.85		9.13	0.93	8.42	0.85
N-10	1.14*	1.35	5.00	12.30		13.86	1.13	13.16	1.07
N-11	0	2.16	7.00	13.55	Shear pressure	12.09	0.89	12.09	0.89
N-12	0.121	2.37	7.50	15.00		12.20	0.81	12.78	0.85
N-13	0.242	3.55	10.00	15.00		12.18	0.81	13.23	0.88
N-14	0.363	3.21	10.63	15.30		11.87	0.78	13.45	0.88
N-15	0.484	3.72	10.62	13.75	Pressure shear brittleness	12.24	0.89	14.34	1.04
N-16	0	2.19	5.00	7.25	Shear pressure	3.24	0.45	5.33	0.73
N-17	0.109	3.37	7.50	12.30		4.40	0.35	7.77	0.63
N-18	0	2.36	5.62	9.0?		4.61	0.51	7.60	0.84
N-19	0.327	3.37	9.38	13.12	Pressure shear	4.52	0.34	9.18	0.70
N-20	0.436	4.78	10.00	14.38		4.50	0.31	9.51	0.66
N-21	0.170	5.40	12.50	17.50	Localized damage	15.62	0.89	18.22	1.04
N-22	0.170	2.03	6.88	17.15	Shear pressure	16.09	0.94	16.29	0.95
N-23	0.170	2.70	8.75	18.75		15.79	9.84	17.19	0.92
N-24	0	2.03	6.60	16.25		16.04	0.99	16.04	0.99
N-25	0	2.37	6.88	11.88	Shear pressure	7.14	0.63	11.77	0.99
N-26	0.090	2.70	8.15	14.25		6.80	0.48	11.91	0.84
N-27	0.180	3.37	11.25	16.88		7.32	0.44	13.47	0.80
N-28	0.279	3.72	11.88	18.75	Pressure shear	7.05	0.38	13.72	0.74

* 1.16 and 1.14 are respectively the N/R_1bh values of the structural components N-9 and N-10

Table 2b. Experimental Results of the Eccentric Pressure Shear and Eccentric Pulling Shear of the Second Batch of Test Components

Number	$\frac{N}{R_l bh}$*	Experimental results** M_f^s (T.M)	Q_f^s (T)	Q_p^s (T)	Form of breaking	Calculated according to the normal method Q_p'	Q_p'/Q_p^s	Calculated according to the suggested method Q_p''	Q_p''/Q_p^s
1	0	2.13	6.88	11.05	Shear pressure	12.76	1.15	12.76	1.15
2	-0.884		3.75	9.70		13.10	1.35	12.72	1.31
3	-1.578		3.25	11.05	Shear pulling	12.87	1.16	12.17	1.10
4	-1.746		5.30	9.10	Shear pressure	12.67	1.39	11.91	1.30
5	0	2.32	5.85	12.35	Shear pressure	13.20	1.07	13.20	1.07
6	-1.030		4.49	11.25		13.42	1.19	12.91	1.15
7	-1.557		3.75	11.70		13.23	1.13	12.46	1.06
8	0	2.25	4.55	10.65	Shear pressure	11.72	1.10	11.72	1.10
9	-1.458		3.75	9.80	Shear pulling	11.89	1.21	11.33	1.16
10	-2.030		5.00	10.30		11.70	1.14	10.93	1.06
11	+0.267	3.56	7.50	14.38	Pressure shear explosive	11.66	0.81	12.43	0.86
12	+0.260	5.60	11.25	16.55		11.53	0.70	13.43	0.81
13	+0.251	3.56	6.88	13.45	Shear pressure	11.89	0.88	12.26	0.91
14	+0.272	2.73	7.20	11.25		11.50	1.02	12.27	1.09
15	+0.437	5.12	9.38	14.15	Pressure shear explosive	10.18	0.71	12.08	0.85
The two batches totalled 43 test components:					Average value $\bar{x}$		0.815		0.931
					Mean square error σ		0.298		0.170
					Scattering percentage cv		0.366		0.183

* The longitudinal forces of the test components Nos. 11-15 listed in the table are pressure, therefore in column No 2 the listed figures for these 5 test components are the corresponding $N/R_a bh$.

**"In the column of "experimental results," M_f^s, Q_f^s, and Q_p^s are respectively the bending moment at the time of occurrence of the perpendicular crack, the shear at the time of occurrence of the slanted crack and the shear at the time the oblique section breaks.

Beams are subjected to axial pull split before horizontal forces were applied (the cracks and the beam axis were perpendicular), and the beam was nearly split through. Because the longitudinal steel reinforcements in the beam were mostly in the pulled area, and there were very few longitudinal steel reinforcements in the pressured area, therefore, the cracks at the top of the beam were wider, and the closer to the other side the narrower the crack. But, under horizontal forces, the cracks at the top part of the beam caused by axial pull gradually closed. Axial pull reduced the resistance to cracking of the perpendicular section and the oblique section, hastened extension of the cracks, the extension of the cracks became longer, therefore, axial pull reduces stiffness of the beam.

The experimental beams were mostly broken by shear pressure, i.e., after the slanted cracks had extended more severely and after the hoop reinforcements reached the yielding point, the stress of the concrete in the area of shear pressure in the beam reached the limit of the strength of pressure resistance and the beam broke. In addition, several beams broke from pressure shear forces, i.e., before the slanted cracks fully widened, they suddenly became horizontal cracks, and characteristics similar to the breaking of columns under pressure occurred, and this was immediately followed by rapid crushing of the concrete in the shear pressure area. This type of breaking occurred in beams with a higher axial pressure rather suddenly. Because it was similar to the breaking of columns under pressure, therefore we have temporarily called this type of sudden explosive shear breaking as "pressure shear breaking" to differentiate it from "shear pressure breaking." In the experiment, there were also individual beams (N-21) that showed localized damage at the point of loading (discussed later in this article).

2. Occurrence of Cracks and Its Relationship With Axial Force

Figures 3 and 4 give the corresponding loads at the time of occurrences of the perpendicular cracks and slanted cracks and their relationship with the axial force. The black dots, the hollow dots and the triangles respectively represent the experimental beams with a shear-span ratio of 1.7, 2.5 and 2.35.

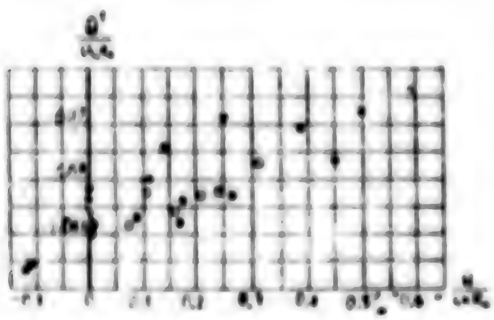

Figure 3. Relationship Between Shear Force and Axial Force at Time of Ocurrence of Perpendicular Crack

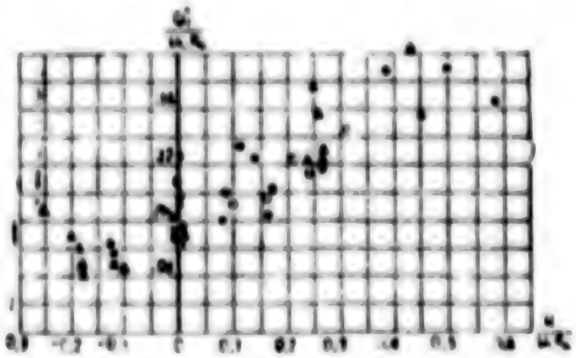

Figure 4. Relationship Between Shear Force and Axial Force at Time of Ocurrence of Slanted Cracks

It can be seen from the diagram that regardless of whether it was a perpendicular crack or a slanted crack, when they occurred, the loads all increased as the axial pressure increased. Also, the loads decreased as the axial pull increased.

And, it can be seen from Tables 2a and 2b that although axial force visibly affects bending and splitting shear force and the slanted pulling and splitting shear force, it does not visibly affect the increments of shear force between the bending and splitting forces and the slanted pulling and splitting forces.

3. Shear Strength and Its Relationship With the Axial Force

Figure 5 shows the relationship of the shear strength and the axial force in the two batches of experimental structural components.

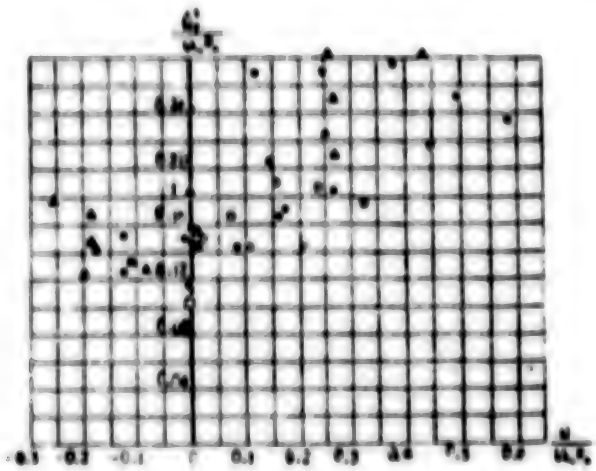

Figure 5. Relationship Between Shear Strength and Axial Force

It can be seen from the diagram that the shear strength of the beam is greatly affected by the axial force. Regardless of whether it is a belly reinforced beam or not, its shear strength increases as the axial pressure increases. This is because axial pressure can delay the formation of slanted cracks, reduce widening of the slanted cracks and increase the height of the shear pressure area of concrete (Figure 9). Therefore, at the time of breaking, the portion of the shear strength borne by the shear pressure area of the concrete increases.

In addition, experiments also prove that the beam's shear strength and the portion of increased shear strength produced by axial pressure all decrease as the shear-span ratio increases.

Here we must describe the beam under axial pull (especially beams without belly reinforcement). For example, beam N-9 that was not belly reinforced was subjected to shear force and axial pull simultaneously, and before applying shear force, the section near the support within the beam's shear-span range and the section near the loading point had all basically split through. Therefore, people will doubt whether this beam can effectively bear horizontal forces or not. The experiment showed after applying axial force, slanted cracks were formed during the course of applying shear force and corresponding bending moment. On the other hand, the upper part of the original pulled crack near the point of exertion of horizontal force gradually closed up, and it did not visibly affect the strength of the experimental beam. At the same time, the cracks caused by axial pull on the section near the support did not close up because of a decrease in the bending moment but because of the gripping strength of the aggregate and the function of the hidden tips of the longitudinal reinforcements. That section can still effectively carry shear force without becoming a broken section.

The effect of eccentricity of the longitudinal pressure upon the shear strength of the beams of the IV group of the first batch and the fourth and fifth groups of the second batch was tested by experiment. Among the beams of the IV group, beam N-24 was not subjected to axial force, the other three beams had the same longitudinal pressure, but the pressure points were different: The longitudinal pressure of beam N-21 was in the pulled area (e_0 = +6.8 cm), the longitudinal pressure of beam N-22 was in the pressured area (e_0 = -6.0 cm), the longitudinal pressure of beam N-23 was on the axial line of the beam (e_0 = 0). The experimental results showed the position of the point of longitudinal pressure greatly affected the formation of the perpendicular cracks and the slanted cracks and the shear strength in the beam (see Table 2). Except for beam N-21 which showed localized damage near the point of longitudinal pressure, obviously, the effect of the longitudinal pressure applied on the pulled side of the structural component was the best.

It can be seen from the experimental results of the two batches of beams that the effects of axial pressure and axial pull upon the shear strength of the structural component subjected to bending can be separately described by two straight lines with different inclinations. The straight line representing the effects of axial pressure had a greater inclination while the straight line representing the effects of axial pull had a smaller inclination. It seems that the effect of axial pressure upon shear strength is higher than axial pull. But we believe: the favorable effect of axial pressure should not be given too much consideration because: (1) under a stronger axial pressure, the structural component will suddenly produce explosive pressure shear and break, and when the axial pressure is higher than a certain limit, it will cause a drop in the shear strenght; (2) structural components under combined pressure, bending force and shear force, when considering the effects of seismic forces, can become structural components under pulling, bending and shear forces, i.e., the favorable effect of pressure may decrease and even become an unfavorable effect.

Therefore, we believe, the effects of axial pressure and pull upon the shear strength of structural components can be uniformly considered, and can be calculated by the principles and the methods described in "suggestions on design."[4] The Q_y in related equations in (4) is changed to Q_N, i.e.:

$$Q_p = Q_{Kh} \pm Q_N \tag{1}$$

while $Q_N = 0.07\,N$ (when calculating Q_{Kh} m is not taken into consideration)

or $Q_N = \frac{0.12}{m}\,N$ (when calculating Q_{Kh} m is taken into consideration) (2)

In equation (1), the sign before Q_N is positive when the axial force is pressure, conversely, it is negative when the axial force is a pulling force.

The calculations for the 43 experimental structural components described above show that the calculated value of the shear strength according to the suggested equations (1) and (2) taking the effect of axial force into consideration

coincides more with the experimental results than the value computed by the standard method not taking the effect of axial force into consideration. Comparing the experimental results and the computed values according to the standard method: $\bar{X} = 0.815$, $\sigma = 0.298$, $c_v = 0.366$; and according to the suggested method: $\bar{X} = 0.931$, $\sigma = 0.170$, $c_v = 0.183$.

4. The Effect of Hoop Reinforcements

It was discovered in the experiment that when only the axial force was acting on the beam, the hoop reinforcement inside the beam basically was not subjected to any force. When the beam was simultaneously subjected to axial force and a horizontal force that was not too large, the stress in the hoop reinforcement in the beam was also very small. Only until slanted cracks emerged in the beam did the stress of the hoop reinforcement suddenly increase visibly and the stress of the hoop reinforcement continued to increase as the horizontal force increased. At the time the beam broke under shear forces, the stress of the hoop reinforcement through the slanted cracks in the beam had basically reached the yielding point (Figure 6). Also, the experiment showed that the effect of belly reinforcement in the beam i.e., the part of the shear force it bore, seemed to be unrelated to the strength of the axial force and its direction. For example, the differences of the shear strengths between group I of beams with belly reinforcements and group II of beams without belly reinforcements under different axial pressures showed almost the same difference as listed in Table 2. Also, for example, the difference between the shear strengths of the beam N-10 with hoop reinforcement and the corresponding beam N-9 with belly reinforcement both subjected to axial pull was 2.55^T; while difference between the shear strengths of the N-12 beam (with hoop reinforcement) and beam N-17 (without hoop reinforcement) under an axial pressure of 7.5^T was also 2.50^T. Here, such a problem may almost come about: From the point of view of the main stress, the angle between the slanted crack and the axis of the beam when the beam is subjected to axial pull will be larger. The angle between the slanted crack in the beam and the structural component when the beam is subjected to axial pressure will be smaller. If this is true, then in the beam subjected to axial pull, the slanted crack will pass through by the crack in beams subjected to axial pressure. But, the experiments have preliminarily shown that on the one hand, the axial force does not greatly affect the inclination of the slanted crack, and on the other hand, this effect, which is not too great, will be canceled by the effect of the height of the shear pressure area. Because the axial force affects the inclination of the slanted crack as well as the height of the shear pressure area at the end of the slanted crack at the same time, and these two affect the projected length of the slanted section and the number of hoop reinforcements being passed through in opposite ways. At the same time, it can be seen from Figure 6 that when the beam breaks due to shear forces when there is axial pull, when there is no axial force and when there is axial pressure, all hoop reinforcements yield. Therefore, the effect of the hoop reinforcements in the beam does not visibly change according to whether an axial force exists or not. This means, axial force does not visibly affect that part of the shear force borne by the hoop reinforcement in the beam.

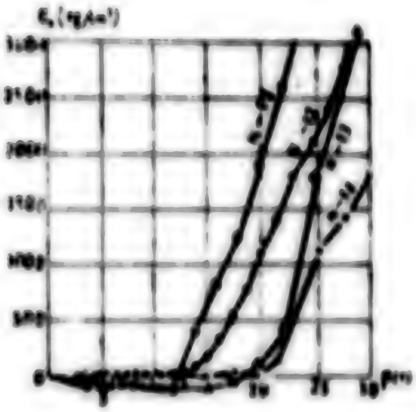

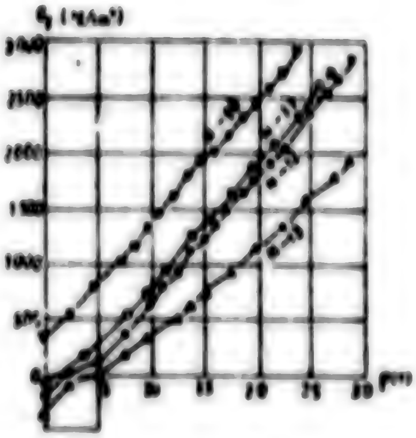

Figure 6. Relationship Between the Stress of the Hoop Reinforcement and External Load

Figure 7. Relationship Between the Stress of the Longitudinal Reinforcement and External Load

In addition, it can be seen from the diagram that even when the beam breaks due to shear forces, the stress of the hoop reinforcements in the beam always reaches the yielding point when there is axial pull, when there is no axial force and when there is axial pressure. But, at each load level (especially the utilization level), the differences in the stress are still very large, therefore, the effect upon widening the slanted cracks is obvious.

5. Stress of the Longitudinal Reinforcements

In the experiment, the stress of the longitudinal reinforcement of each beam was measured. Figure 7 shows the variation of the stress of the longitudinal reinforcement in the mid span section along with different loads in the N-10 beam subjected to an axial pull of 10^T, the N-11 beam subjected to no axial force and the N-12 and N-13 beams subjected to axial pressures of 7.5^T and 15^T. It can be seen that the stress of the longitudinal reinforcement is related to the strength and the direction of the axial force. Axial pull causes the stress of the longitudinal reinforcement to increase. Axial pressure causes the stress of the longitudinal reinforcement to drop. The higher or lower stress of the longitudinal reinforcement also affects the effect of the hidden tip of the longitudinal reinforcement, therefore, beams subjected to axial pressure have a greater shear bearing ability because of a better effect of the hidden tip of the longitudinal reinforcement.

Table 3 lists the actually measured values of the stress of the longitudinal reinforcement of the mid span section and the intermediate section between shear and span near the time when the beam breaks due to shear forces in four beams. It can be seen from the table that the stress of the longitudinal reinforcement of these two sections are very close. Therefore, they once again show that near the time when the beam breaks due to shear force, the reinforced concrete beam has gradually changed into "an arch with a pulled rod."

Table 3. Stress of the Longitudinal Reinforcement of the Intermediate Section Between Shear and Span and the Mid Span Section of the Beam at the Time Near the Breaking of the Beam by Shear Forces

	Longitudinal stress (kg/cm^2)	
Number of beam	Mid span section	Intermediate section between shear and span
N-10	2900	2850
N-11	2690	--
N-12	2840	2640
N-13	1940	1780

6. Width of Slanted Crack

Figure 8 shows the relationship between the external load and the widening (at the center of the height of the section) of the slanted crack in the beams of group I with belly reinforcements. It can be seen from the diagram that whether axial forces exist or not and the strength and direction greatly affect the load causing slanted cracks to occur and the stress of the hoop reinforcement. These also affect the width of widening of the slanted crack. Ordinarily, under an operating load, the width of slanted cracks in beams subjected to axial pressure is narrower while the width of the slanted cracks in beams subjected to axial pull is wider.

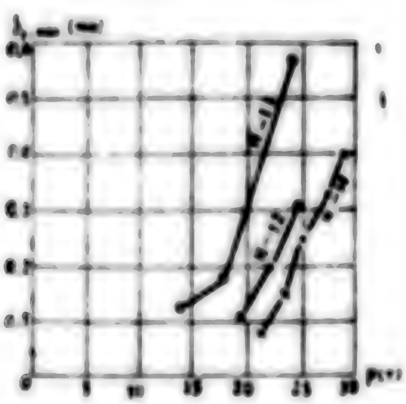

Figure 8. Relationship Between Width of Slanted Crack and External Load

In addition, the shape of the widening of the slanted crack in the beam does not seem to be closely related to whether there is an axial force or not. The shapes of the cracks in the experimental beams were basically the same. They were all widest at the center of the height of the section, followed by cracks at the horizontal position of the pulled longitudinal reinforcement and the narrowest at the tip of the slanted crack.

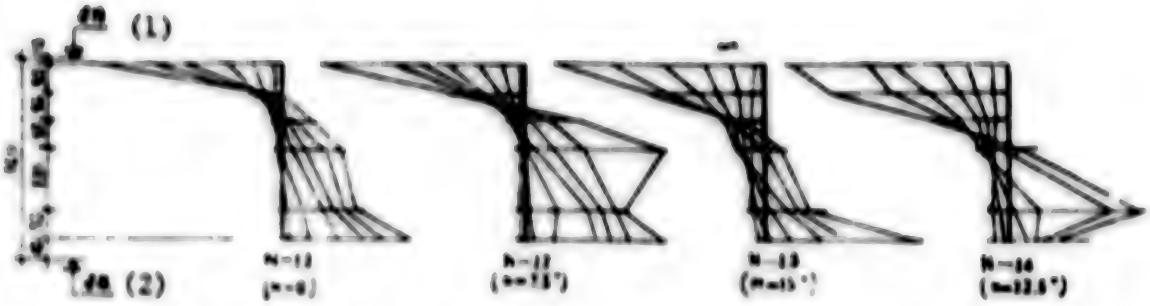

Figure 9. Relationship Between Distribution of Stress of the Section and Axial Force

Key: (1) Top of beam (2) Bottom of beam

7. Strain of the Section and Its Distribution

Figure 9 shows the average strain and its distribution within the 25 cm section at the mid span actually measured under various loads in the 4 beams N-11, N-12, N-13 and N-14. It can be seen from the figure that although the axial force affects the absolute value of the pressure strain on the fibers of the rim only slightly, it greatly affects the distribution and shape of the strain and the height of the pressured area. In the figure, the differences in the height of the pressured areas of the 4 beams subjected to the same horizontal force of 25T are not small: the height of the pressured area of N-11 (N = 0) was 6.5 cm, that of N-12 (N = 7.5T) was 6.9 cm, that of N-13 (N = 15T) was 10.7 cm, that of N-14 (N = 22.5T) was 11.6 cm. This partially proves that applying axial pressure can increase the height of the shear pressure area of the structural components, and thus, it increases the shear bearing capability of the structural component.

III. Conclusion

1. The experiments showed that the axial force acting on the beam not only greatly affected the shear resistance of the normal section and the oblique section, but also affected the shear strength a lot. The resistance to cracking of the normal section and the oblique section of the reinforced concrete beam and the shear strength of the oblique section increased as the axial pressure increased. Conversely, they weakened when an axial pulling force existed. Therefore, in construction design using structural components that are subjected simultaneously to shear force, bending moment and axial forces, consideration of the effect of axial force upon the shear strength is very necessary.

2. Applying axial pressure increases the ability of the beam to resist shear forces. The reason is that it delays the occurrence and the development of slanted cracks, increases the height of the shear pressure area of concrete at the critical time of splitting, improves gripping among the aggregates and the function of the hidden tip of the longitudinal reinforcement, thus increasing that part of the shear force borne by the concrete in the beam. Conversely, the existence of an axial pulling force reduces the ability of the beam to resist shear.

3. Experiments showed that the function of the belly reinforcements in the beam does not visibly change whether an axial force exists or not. This is because axial force does not greatly affect the inclination of the slanted crack. At the same time, this effect is also canceled by the effect of the height of the shear pressure area or is partially canceled.

4. The effect of weakening the shear strength of the beam by the axial pulling force is not as serious as pointed out in references.[5,6] Also, its effect is smaller than axial pressure. When the axial pulling force reaches and surpasses the anti-pulling strength of the concrete of the section of the structural component, and after splitting, even the beam without the belly reinforcement still has a definite ability to bear a shear load.

5. Comparison of the computed valu[illegible] e experimental results showed that according to the method of the de[illegible]n cou[illegible] (TJ10-74), because the effect of axial forces upon the shear strength of the structural components was not considered, the error was larger, the computed results for the 43 structural components were: $\bar{X} = 0.815$, $\sigma = 0.298$, $c_v = 0.366$. According to the suggested method of this article, i.e., calculating according to equations (1) and (2), the error visibly lessened because consideration was given to the effect of axial forces, thus, $\bar{X} = 0.931$, $\sigma = 0.170$, $c_v = 0.183$.

6. In the future, the effect of axial forces upon the shear strength of structural components should be continually studied. In particular, the problems of the effects of axial forces on the ability of prestressed concrete structural components subjected to bending to resist shear force and the upper and lower limits of the effects of axial forces must be studied to provide a more rational method of calculating the shear strength of the oblique section of eccentrically pressured and eccentrically pulled structural components.

The experimental work for this article received the enthusiastic help from comrades Guo Ruisen [6753 3843 2773] of the Beijing Architectural Engineering Academy and Zhao Guangtian [6392 1684 3944] of the Zhengzhou Engineering Academy. During the course of writing this article, Professor Ding Tajun [0002 1129 6874] provided valuable suggestions. We profoundly thank them here.

REFERENCES

1. ACI-ASCE Committee 426: "The Shear Strength of Reinforced Concrete Members," JOURNAL OF THE STRUCTURAL DIVISION, ASCE, No ST 6, June, 1973 (The translation appears in the printed material of the Nanjing Institute of Technology entitled "Shear Strength of Reinforced Concrete Members," 1974, 5).

2. R. Park, T. Paulay: "Reinforced Concrete Structures," New York, 1975.

3. Special topic research group on shear strength: Limiting conditions of the sections of reinforced concrete structural components subjected to bending and the effect of prestressing upon the shear strength of the oblique section. JIANZU JISHU TONGXUN [ARCHITECTURAL TECHNIQUES BULLETIN (Architectural Structure)], 1978, 4.

4. Special topic research group on shear strength: Suggestion I, the limiting conditions of the sections of reinforced concrete structural components subjected to bending and the suggestion for calculating the shear strength of the prestressed concrete structural components subjected to bending. ARCHITECTURAL TECHNIQUES BULLETIN (Architectural Structure), 1978, 4.

5. A. H. Mattock: "Diagonal Tension Cracking in Concrete Beams With Axial Forces." JOURNAL OF THE STRUCTURAL DIVISION ASCE, No ST 9, Sept 1969.

6. M. J. Haddadin, S. Hong and A. H. Mattock: "Stirrup Effectiveness in Reinforced Concrete Beams With Axial Forces." JOURNAL OF THE STRUCTURAL DIVISION ASCE, No ST 9, Sept 1971.

7. A. S. Zorich: The Apparent Ability To Simply Lengthen Custom-made and Very Strong Concrete Under the Action of Transverse Forces, "Concrete and Reinforced Concrete," 1976, 11.

8. Fifth Department of the Nanjing Institute of Technology, Maanshan 17 Metallurgical Construction Company No 1: Experimental Study of the Effect of Axial Forces Upon the Shear Strength of the Reinforced Concrete Beam (I), 1978, 9.

9296
CSO: 8111/0599B

STIFFNESS, CRACK OF ECCENTRICALLY LOADED STRUCTURAL COMPONENTS

Nanjing NANJING GONGXUEYUAN XUEBAO [JOURNAL OF NANJING INSTITUTE OF TECHNOLOGY] in Chinese No 1, 1980 pp 33-46

[Article by Ding Dajun [0002 1129 6874] and Pang Tonghe [1690 0681 0735: "Experimental Studies of Stiffness and Crack of Eccentrically Loaded Reinforced Concrete Members of Rectangular Sections"*]

[Text] Abstract

Our nation's design code for reinforced concrete structures (TJ10-74) does not include the method of calculating stiffness and crack of eccentrically loaded structural components. This article provides information on the strain on 24 short reinforcements in a rectangular section of reinforced concrete, the whole procedure for calculating the strain of partial test components of concrete bearing a load, and the whole procedure for measuring deflection and curvature. In addition, it also provides measured data of the widths of cracks of large eccentrically loaded test components. Strain measurements show the average strain coincides with the hypothesis of the flat section. A few test components were measured until they broke. Computations show the computational formulas for eccentrically loaded stiffness and cracking suggested in the computational system for stiffness and cracking originally to be included in the codes fit the data better.

In 1977, we had continuously proposed the method of calculating[1,2] the stiffness and cracks of eccentrically loaded structural components based on domestic and foreign information. This experiment is one of the projects carried out in scientific research and planning for the codes and is a part of the work to be done for the entire experimental research plan on stiffness and cracking.

I. Brief Description of the Experiment

The experiment is divided into two groups, separately conducted in October-November of 1978 and June-July of 1979. A total of 24 rectangular section test components of a uniform length of 1.5 m were used. Figure 1 and Table 1 show the dimensions of the test components and the fitted reinforcements. The material characteristics are listed in Table 2. The dimensions of the legs of the first group of test components were c=29.5, 18.5, 14.5 and 0 cm (0 designates small eccentrically loaded structural components).

*This article was received on 28 December 1979.

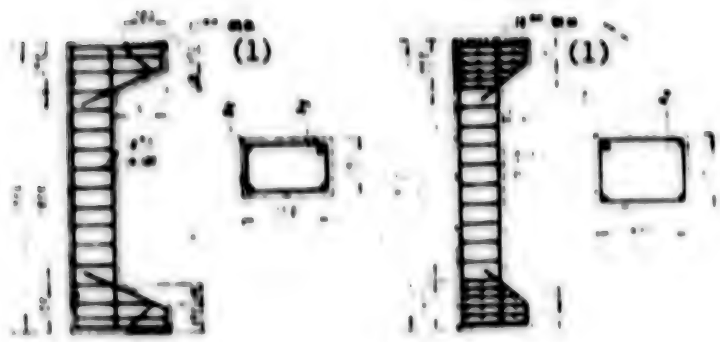

Figure 1. Dimensions of the Test Structural Components and Structure of the Reinforcements

Key: (1) Steel plate

Table 1. Dimensions of the Test Components and Reinforcements

Batch Number	No of Test Component	Dimension of Section mm			Reinforcement	
		b×h	a	a′	A_s	A'_s
First batch	Z−1	150×250	35	31	2Φ20	2Φ12
	2	150×248	32	28	2Φ12	2Φ12
	3	150×251	32	35	2Φ16	2Φ12
	4	151×251	32	35	2Φ16	2Φ16
	5	151×249	31	34	2Φ16	2Φ16
	6	150×250	33	37	2Φ16	2Φ16
	7	151×253	32	37	2Φ20	2Φ20
	8	152×249	25	36	2Φ12	2Φ12
	9	150×253	35	34	2Φ16	2Φ16
	10	151×253	31	30	2Φ8	2Φ8
	11	152×252	33	31	2Φ12	2Φ12
	12	151×253	35	34	2Φ16	2Φ16
Second batch	Z I − 1	179.3×252	37.9	33.1	2Φ12	2Φ12
	2	180.7×252	36.5	42.4	2Φ16	2Φ16
	Z II − 1	180.2×252.3	32.8	41.4	2Φ12	2Φ12
	2	180×251.5	34.4	45.4	2Φ16	2Φ16
	Z III − 1	180.2×252.7	38.5	33.1	2Φ12	2Φ12
	2	180.5×254.3	30.5	45.5	2Φ16	2Φ16
	Z IV − 1	180.8×251.8	37.3	35.4	2Φ12	2Φ12
	2	180.5×253.2	34.0	48.6	2Φ16	2Φ16
	Z V − 1	179.3×252.2	31.9	40.0	2Φ12	2Φ12
	2	179.8×251.3	40.0	40.8	2Φ16	2Φ16
	Z VI − 1	181.7×252.3	35.4	36.5	2Φ12	2Φ12
	2	179.5×251	39.3	40.8	2Φ16	2Φ16

Table 2. Material Characteristics

Batch number	Steel reinforcement					Concrete (kg/cm^2)				Remark
	Dimensions	R_g (kg/cm^2)	R_b (kg/cm^2)	$E_g \times 12^{-6}$ (kg/cm^2)	δ_5 (%)	R	R_a	R_l	$E_h \times 10^{-5}$	
First batch	Φ 8	2540	3710	2.07	—	307	257	24.1	3.793	
	Φ12	3755	5927	2.03	—					
	Φ16	3553	5517	1.994	—					
	Φ20	3750	5657	2.10	—					
Second batch	Φ12	3081	4121	1.90	30.6	313	213	22.4	3.05	For ZI~ZIV
	Φ16	4521	7054	2.126	21.4	272	211	17.0	3.13	For ZV~ZVI

In the second group of test components, the original design of Φ 16 used II grade reinforcements but later III grade reinforcements were used by mistake. The cubic strength and pulling strength of the concrete were determined by testing the resistance to pressure and splitting (using 5 x 5 mm square steel cushions) of 15 x 15 x 15 cm cubic test pieces. R had been multiplied by the coefficient 0.95 and converted. The elasticity modulo and the strength of resistance to pressure of the concrete were determined by experiment using 10 x 10 x 30 cm columns.

For the first group of test components, at the time, consideration was given to conserving steel. The distribution board was only 20 cm wide. The range of strength of the legs or the belly reinforcements at the ends of small eccentrically loaded structural components was not sufficiently strengthened. Thus half of the test components could not be pressured to the point of breaking. Therefore for the second batch of test components, we used full steel plates and greatly strengthened the leg structures.

The columnar test components were subjected to pressure on the 200 t pressure tester. A hand-held extensometer was used to measure the average strain of three segments (25 cm x 3). In the first batch of test components, electrical resistance plates were used to measure the strain of steel reinforcement Ag. In the second batch of test components, the strain of steel reinforcements Ag and A'g and the compressive strain of loaded concrete of seven test components were measured. The strain of 5 test components among them (ZII-1, 2, ZIV-2 and ZVI-1, 2) was measured by the 100-point automatic electrical resistance strain meter. The other two test components (ZV-1, 2) were measured simultaneously by three people on three YJ-5 electrical resistance strain meters. In addition, a percentage table and a vertical deflection frame made of angular steel (with a fixed ream on one side and a movable ream on the other end) were used to measure the deflection at the central part and the two points corresponding to the two outside points measured by the hand held extensometer, i.e., the distance from each point to the center of the structural component was 37.5 cm. This information was used to calculate the average curvature of this segment to check

against the measurements of the hand held extensometer and the curvature computed hypothetically according to the average strain coinciding with that of a flat section.

II. Results of Strain Measurements

Figure 2 shows the diagram of the stress of steel reinforcements calculated from the measured results of the strain of steel reinforcements. It can be seen from the diagram that for large eccentrically loaded structural components, the stress diagram of steel reinforcements generally consists of three straight lines, i.e., there are two breaks where crack occurs and at the time the steel reinforcement yields. The curvature of the stress curve of the loaded steel reinforcement is larger. In the diagram, the triangular symbol indicates the corresponding load at the time the steel reinforcement yields. Under a large eccentric pressure (including critical eccentric pressure), the stress of the pulled steel reinforcement Ag at time of breaking reaches the yielding point. Of course, in Z-5, Z-6 which could not be pressured to the breaking point, the stress of Ag did not reach the yielding point. But for ZV-1, although it was pressured until it broke, the stress of Ag still did not reach the yielding point. This may be related to the following phenomenon: Because the breaking section was 20 cm from the point of measurement, the width of the horizontal crack of the steel reinforcement reached 1.5 cm, the deformation was overly centralized and the structural component suddenly broke. Under a small eccentric pressure, the stress of Ag reached the yielding point at the time the element was being pulled by the critical eccentricity and the stress gradually lessened and changed into pressure. Regardless of whether the eccentric pressure is large or small, at the time of breaking, the stress of the pressured steel reinforcement (six test components) reached the yielding point even when the yielding point of the III grade steel reinforced test components was as high as 4521 kg/cm^2.

Figure 3 shows the εg - $\bar{\varepsilon}g$ curve of some of the large eccentrically pressured test components. The parallel relationship has been generally established, but the others are parallel in another direction. This problem still requires further study.

Figure 4 shows the strain of the pressured concrete test component ZII-1 measured at each point (a total of nine points, the measured length was about 37.5 cm) lengthwise along the central part of the structural component under various loads. It can be seen from the diagram that at the beginning of loading, the distribution of strain was less even, but as the load increased, the distribution of strain expanded. The largest strain corresponded basically to the positions of cracks. At the time of breaking, most of the test components showed an average strain surpassing 3.5 percent within the range of measurements.

It should be pointed out that when the moment of breaking was near or reached, the strain of the concrete lessened. This may be due to redistribution resulting from deformation, i.e., the strain at some points increased while that at some other points decreased. But during the latter period, the decrease in the strain at all points may be related to the fact that the concrete had been crushed or the cement had loosened as a result of the occurrence of many small cracks (electrical resistance plates).

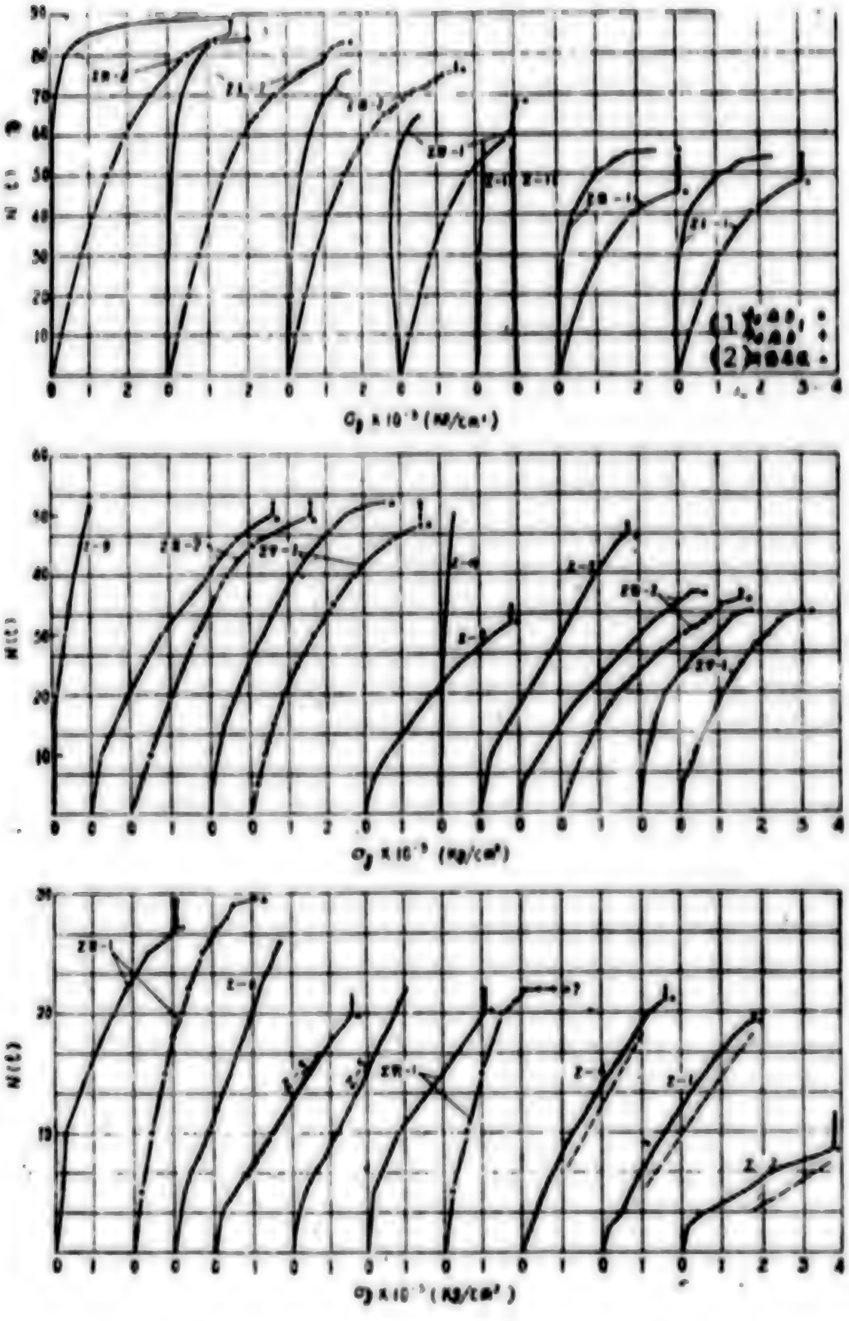

Figure 2. Diagram of Stress of Steel Reinforcements

Key: (1) Stress (2) Yielding of steel reinforcements

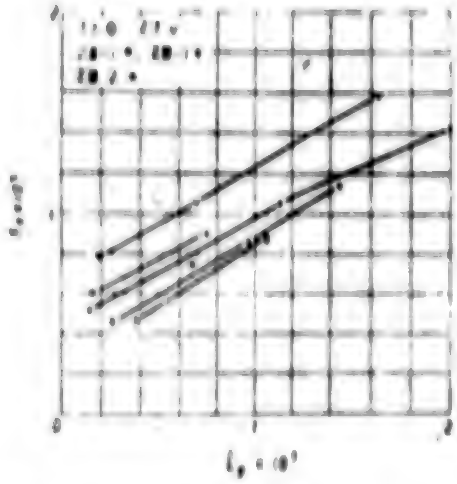

Figure 3. ε_g - $\tilde{\varepsilon}_g$ Relationship Curve

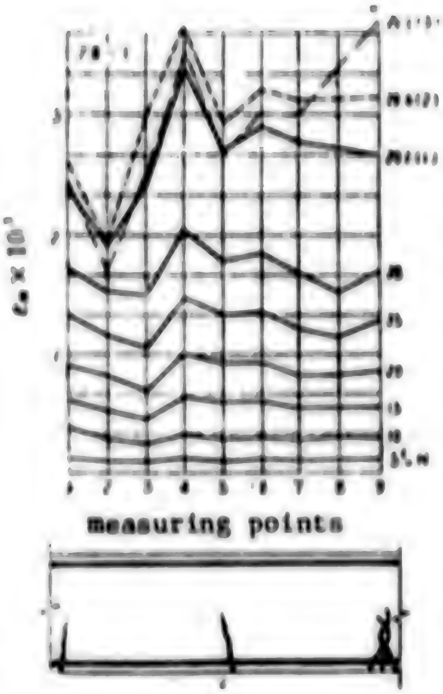

Figure 4. Presure Strain at the Concrete Rim

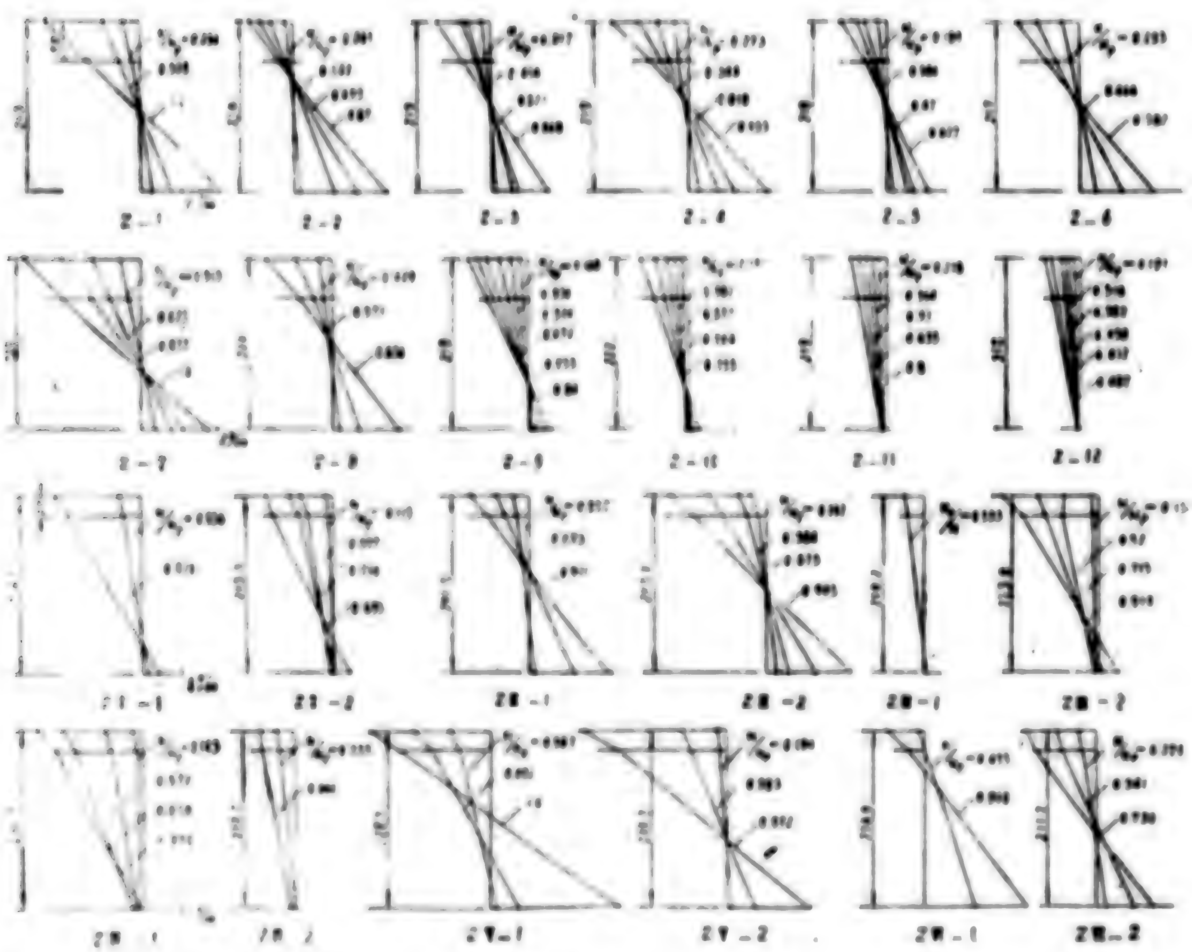

Figure 5. Distribution of Strain Along the Height

Figure 5 shows the entirety of the distribution of the average strain along the height of the section. It can be seen that the average strain basically coincides with the hypothesis of the flat section. Here, three test components (Z-1, Z-7 and ZV-1) were measured until they broke ($N/N_p = 1.0$). This can be used as the experimental basis for the computational model of the flat section hypothesis used in calculations of strength because breaking actually also occurs within one segment.

III. Experimental Results of Deflection and Curvature and Their Analysis

Although the structural components were 150 cm long, but because of the installation of the deflection frame, our measured deflection was actually that of a 138 cm long structural component, i.e., equivalent to the deflection value with A,B as the supporting points (Figure 6). Because of the necessity of adding the load, legs were added to the two ends of the structural component. This greatly increased the stiffness of this area, therefore the side shifts of points D and E were measured at the same time and thus the deflection Δf within the length of the structural components as equal sections was also given. In this way, the average stiffness of this segment can be more accurately examined.

According to the principles of mechanics, it is not difficult to prove that in symmetry, the deflection between D and E can be determined by the simple supporting structural components at Δf the two ends bearing a bending moment of Ne_0.

Figure 7(a)(customarily, the diagram shows the structural component in a lying position) shows the M/B diagram of any symmetrically loaded structural component. According to the conjugate beam method, we have:

$$f_C = M_C^* = M_D^* + Q_D^* \cdot \overline{DC} - \int_0^{\overline{DC}} \frac{M}{B} dx (\overline{DC} - x)$$

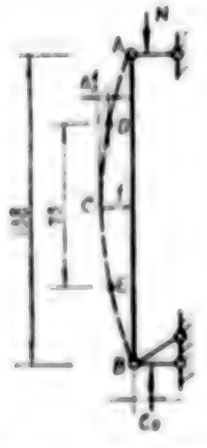

Figure 6. Illustration of Eccentric Pressure

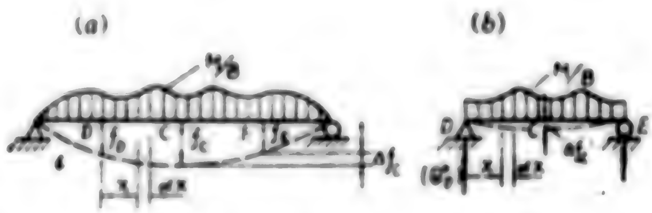

Figure 7. Conjugate Beam

where: M_C^*, M_D^* and Q_D^* --- are respectively the bending moment and the shear at points C and D on the conjugate beam. Because $M_D^* = f_D$, thus:

$$\Delta f_C = f_C - f_D = Q_D^* \cdot \overline{DC} - \int_0^{\overline{DC}} \frac{M}{B} dx (\overline{DC} - x)$$

From Figure 7(b), we have $\Delta f_C = (Q_D^*)\overline{DC} - \int_0^{\overline{DC}} \frac{M}{B} dx(\overline{DC} - x)$

and when $\frac{M}{B}$ is symmetric, $(Q_D^*) = Q_D^*$, thus:

$$\Delta f_C = \Delta f'_C$$

i.e., Δf_C can be calculated when D and E are taken as the simple supports (but the D and E ends bear the sectional bending moments of the original structural component).

The curves of the deflection Δf for the 24 test components measured are shown in Figure 8.

The experimental values of the curvature were determined by two methods.

(1) According to the hypothesis of the average strain of the flat section:

$$\left(\frac{1}{\rho}\right)_1 = \frac{\bar{\varepsilon}_h^s - \bar{\varepsilon}_g^s}{h_0} \qquad (1)$$

where: $\bar{\varepsilon}_h^s$, $\bar{\varepsilon}_g^s$ --are respectively the average strain of the concrete at the rim of the pressured area (or greater pressure) of the structural component measured and the average strain of the steel reinforcement Ag. When the steel reinforcement is pulled, it takes a negative sign and when it is pressured it takes a positive sign.

(2) According to the arc of the deformation curve among DCE, we have:

$$\left(\frac{1}{\rho}\right)_2 = \frac{2\Delta f}{\overline{DC}^2} \qquad (2)$$

and we take the average value of $\left(\frac{1}{\rho}\right)_1$ and $\left(\frac{1}{\rho}\right)_2$ calculated in equations (1) and (2) as $\left(\frac{1}{\rho}\right)_s$, i.e.:

$$\left(\frac{1}{\rho}\right)_s = \frac{1}{2}\left[\left(\frac{1}{\rho}\right)_1 + \left(\frac{1}{\rho}\right)_2\right] \qquad (3)$$

Table 3 gives the measured values and the computed values of the deflection and the average curvature of the DE segment under two grades of loads.

It can be seen from Table 3 that except for a few cases, in general, $\left(\frac{1}{\rho}\right)_1$ and $\left(\frac{1}{\rho}\right)_2$ are close, and they are similar to the results of our past experiments of structural components subjected to bending.[3]

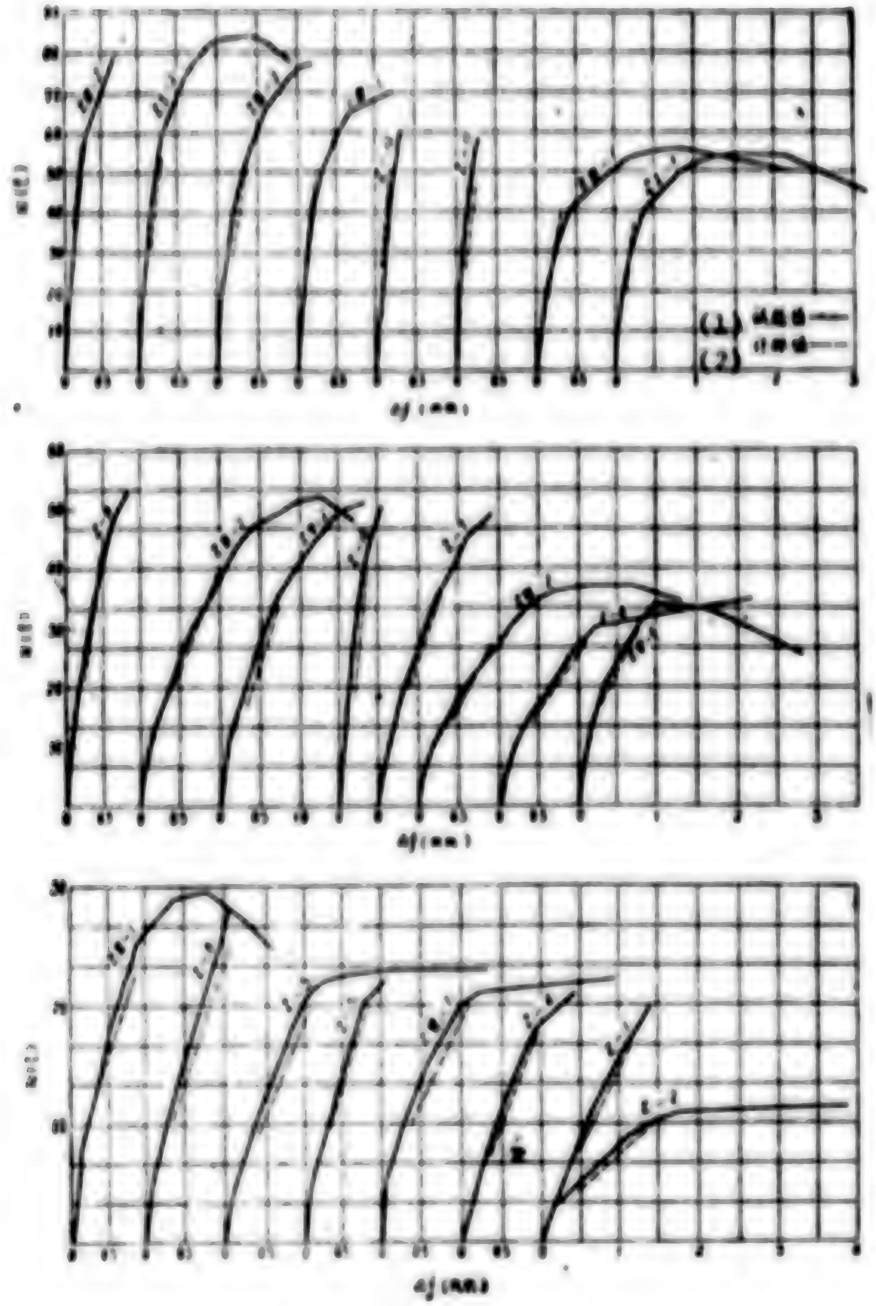

Figure 8. N-Δf Curve

Key: (1) Experimental values
(2) Computed values

Table 3. Comparison of the Measured Values and the Experimental Values of the Deflection and the Curvature

No of test components	Load N (t)	Eccentric distance e_0 (cm)	Deflection Δf_0 (mm)	Δf (mm)	$\Delta f_0/\Delta f$	f_0 (mm)	f (mm)	f_0/f	Curvature $(\frac{1}{\rho})_1$ (10^{-6}/mm)	$(\frac{1}{\rho})_2$ (10^{-6}/mm)	$(\frac{1}{\rho})_0 = \frac{1}{2}[(\frac{1}{\rho})_1 + (\frac{1}{\rho})_2]$ (10^{-6}/mm)	$(\frac{1}{\rho})$ (10^{-6}/mm)	$(\frac{1}{\rho})_0 / (\frac{1}{\rho})$
Z—1	9.0 12.0 (10.0)	31.8	0.51 0.715	0.566 0.785	0.900 0.911	1.95 2.83	1.915 2.65	1.02 1.068	(7.18	8.33	8.06	9.07	(0.8[illegible])
2	6.0 8.0	31.9	0.64 0.95	0.744 1.075	0.862 0.884	2.075 3.105	2.515 3.63	0.826 0.857	7.90 11.60	9.12 13.5	8.51 12.55	10.58 15.30	0.805 0.822
3	12.0 16.0	20.8	0.48 0.71	0.592 0.835	0.812 0.852	1.76 2.185	2.00 2.82	0.88 0.775	6.78	6.84	6.81	8.42	0.810
4	11.0 (12.0) 15.0	20.8	0.472 0.711	0.530 0.775	0.892 0.918	1.691 2.500	1.79 2.62	0.944 0.955	(7.06	7.48	7.27	8.37	(0.87[illegible])
5	15.0 20.0	16.9	0.535 0.760	0.565 0.803	0.948 0.946	1.845 2.768	1.91 2.715	0.964 1.020	6.82 10.42	7.62 1.082	7.22 10.62	8.06 11.42	0.895 0.930
6	20.0 25.0	17.1	0.690 0.935	0.815 1.058	0.846 0.885	— —	2.00 2.57		10.25	13.3	11.78	11.6[illegible]	1.014
7	25.0 30.0	13.1	0.455 0.575	0.484 0.607	0.944 0.948	— —	2.26 2.82		9.05	8.2	8.63	8.6	1.035
8	17.0 22.0 (20.0)	13.0	0.484 0.736	0.538 0.772	0.900 0.955	1.502 2.418	1.82 2.61	0.823 0.925	(7.51	9.33	8.42	9.28	(0.9[illegible])
9	30.0 40.0	8.2	0.315 0.475	0.324 0.440	0.972 1.080	1.115 1.750	1.095 1.485	1.02 1.178	4.42 6.73	4.49 6.76	4.46 6.75	4.62 6.27	0.965 1.075
10	27.0 (30.0) 35.0	6.6	0.185 0.270	0.257 0.343	0.720 0.788	0.612 0.940	0.867 1.16	0.706 0.810	(4.74	3.06	3.90	4.10	(0.952)
11	35.0 45.0	4.4	0.125 0.180	0.165 0.212	0.757 0.850	0.535 0.732	0.557 0.715	0.960 1.023	2.14 2.85	1.78 2.57	1.96 2.71	2.35 3.02	0.833 0.8[illegible]8

[continued]

[Table 3--continued]

12	35.0 (36.0) 45.0 (48.0)	3.9	0.150 0.198	0.13 0.166	1.152 1.173	0.555 0.782	0.439 0.56	1.267 1.392	(2.35 (3.39	2.21 3.17	2.28 3.28	1.92 2.58	1.1[illegible] 1.27[illegible]
ZI—1	25 30	5.0	0.143 0.185	0.150 0.181	0.955 1.022	0.475 0.620	0.506 0.612	0.940 1.010	3.07	2.64	2.86	2.58	1.110
2	40 50	5.0	0.167 0.279	0.211 0.265	0.792 1.052	0.532 0.732	0.713 0.895	0.748 0.820	3.57	3.97	3.77	3.77	1.0[illegible]
ZII—1	18 22(20)	13.0	0.505 0.723	0.625 0.835	0.807 0.867	1.600 2.350	2.110 2.820	0.758 0.834	(8.72	9.12	8.92	10.28	0.87[illegible])
2	30 38(35)	12.0	0.660 0.970	0.685 0.915	0.965 1.060	2.020 2.875	2.310 3.190	0.875 0.902	(12.02	12.6	12.31	11.78	1.052)
ZIII—1	30 35	6.0	0.235 0.325	0.236 0.276	0.998 1.176	0.71 0.99	0.798 0.935	0.890 1.058	2.73	3.35	3.04	3.35	0.9[illegible]
2	40 50	6.0	0.21 0.32	0.261 0.328	0.805 0.975	0.68 0.87	0.882 1.108	0.771 0.786	3.50	3.0	3.25	3.71	0.876
ZIV—1	35 40	4.0	0.1675 0.200	0.154 0.177	1.088 1.130	0.52 0.63	0.521 0.597	0.997 1.052	3.47	2.85	3.16	2.51	1.250
2	45(30) 50	4.0	0.202 0.233	0.180 0.200	1.120 1.165	0.545 0.64	0.609 0.676	0.895 0.945	(2.0	1.71	1.68	1.71	1.100)
ZV—1	20 25	10.0	0.318 0.504	0.392 0.511	0.812 0.986	1.03 1.62	1.32 1.73	0.782 0.937	5.2	4.53	4.87	5.6	0.872
2	25 30	11.0	0.4 0.55	0.518 0.643	0.772 0.857	1.26 1.72	1.75 2.17	0.720 0.793	8.22	7.85	8.04	9.15	0.880
ZVI—1	15 20	15.0	0.563 0.925	0.745 1.073	0.757 0.862	1.908 3.158	2.52 3.64	0.757 0.870	16.0	13.2	14.6	15.3	0.955
2	18(20) 22	14.0	0.475 0.735	0.554 0.705	0.858 1.040	1.68 2.36	1.87 2.38	0.898 0.990	(8.5	8.55	8.53	8.95	0.955)
Average $\Delta f_e/\Delta f$ Mean square error σ Scattering percentage C_v					0.937 0.134 0.143			0.911					0.966 0.120 0.124

Figure 9 also illustrates the whole procedure for calculating $\frac{1}{\rho}$ according to equation (2) for the four large eccentrically pressured test components.

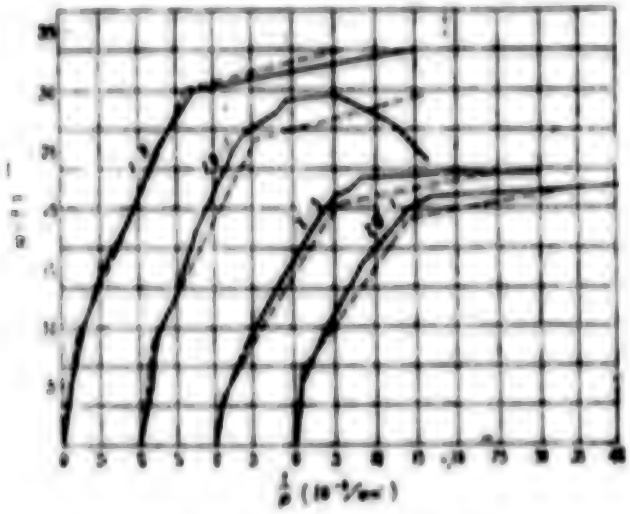

Figure 9. $N - \frac{1}{\rho}$ Curve

When $e_0/h_0 > 0.55$, the computed stiffness of the (rectangular section) structural component can be determined by the following equations[1,2]:

$$B_d = \frac{E_g A_g h_0^2}{\psi(1.15 - 0.3\frac{h_0}{e_0}) + 0.2 + 6n\mu} \tag{4}$$

$$\psi = 1.2\left[1 - \frac{0.235bh^2R_f}{M(1 - 0.3\frac{h_0}{e_0})}\right] \tag{5}$$

When $e_0/h_0 \geq 0.15$, the stiffness of the structural component is determined by the following equation:

$$B_d = 0.85E_h J_0 \tag{6}$$

When e_0/h_0 is between 0.15 and 0.55, we interpolate using equations (4) and (6).

The measured values and the computed values of ψ are compared in Figure 10. Its average value and computed value are relatively close. (The computed strain of the steel reinforcement is determined by σ_g calculated from equation (11), see next section.)

In reference (1), the value corresponding to $\frac{n\mu}{\zeta}$ of equation (4) is taken in the following form:

$$\frac{n\mu}{\zeta} = \frac{0.2 + 6n\mu}{(1 + 2\gamma')(1 + 0.45\frac{h_0}{e_0})} \tag{7}$$

For the rectangular section, we take $\gamma' = 0$.

$$\left(\frac{n\mu}{\zeta}\right)_s = \frac{E_s A_s h_0 \bar{\varepsilon}_s}{Ne} \quad (8)$$

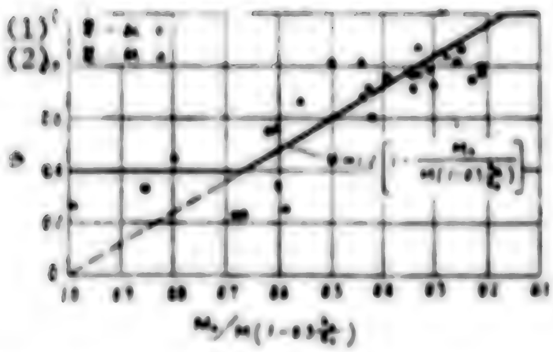

Figure 10. ψ Experimental Value

Key: (1) First batch
(2) Second batch

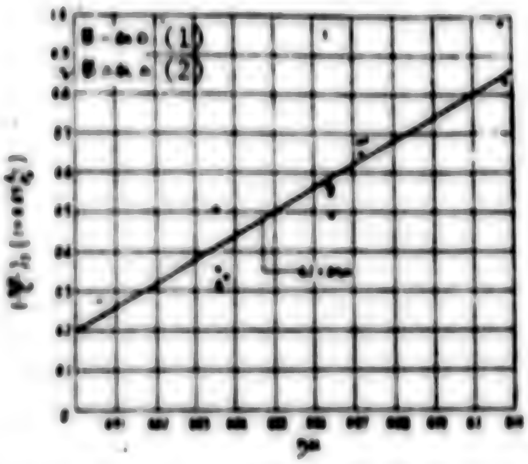

Figure 11. $\left(\frac{n\mu}{\zeta}\right)_s$ Experimental Value

Key: (1) First batch
(2) Second batch

Figure 11 shows the curve of the coefficients of comprehensive deformation of the pressured rim of the concrete. For the 14 test components (large eccentric pressure or close to large eccentric pressure),

$\left(\frac{n\mu}{\zeta}\right)_s / \left(\frac{n\mu}{\zeta}\right) = 0.762 - 1.100, 1.245$, the last ratio corresponds to the test component when $e_0/h_0 = 0.455$. At this time, the stiffness should actually be calculated by interpolation. The average

$\left(\frac{n\mu}{\zeta}\right)_s / \left(\frac{n\mu}{\zeta}\right) = 0.955$.

Deflection is calculated according to the following equation:

$$f = 0.125 \frac{Ne_0 H^2}{B_s} \quad (9)$$

Here, because the length of the structural component is shorter, the added effect of an increase in the bending moment caused by deflection is not taken into consideration.[1,2]

In Table 3, the average $\Delta f_s/\Delta f = 0.937$, $\sigma = 0.134$, $C_v = 0.143$. Coincidence is acceptable but they are more dispersive than the data statistically obtained for structural components subjected to bending in the past (those for the latter are 0.963, 0.1125 and 0.117), $\left(\frac{1}{\rho}\right)_s / \left(\frac{1}{\rho}\right) = 0.966$, $\sigma = 0.120$, $C_v = 0.124$.

The average $f_g/f = 0.911$, smaller than $\Delta f_g/\Delta f$, but the two batches respectively average 0.951 and 0.876, their average $\Delta f_g/\Delta f = 0.911$ and 0.959, i.e., the average of the first batch f_g/f is larger than the average $\Delta f_g/\Delta f$. This should be related to the drastic drop in stiffness of that part after the legs cracked. It can be seen from the table that $\Delta f_g/\Delta f$ and the average values of $(\frac{1}{\rho})_g/(\frac{1}{\rho})$ are close. In the first batch of test components, because there were more slanted and verticle cracks in the legs, such as test components Z1, Z3, the stiffness within the range of the legs also decreased a lot, therefore f_g/f was larger than $\Delta f_g/\Delta f$. In Z6 and Z7, because the percentage table near the two end installations was out of order, measurements were not shown (for the second batch of structural components, the deflection frame was reamed on both ends of the test component but for the first batch of test components, the point of support of the ream was farther away from the end of the test components, therefore the shifts of the two ends were measured--actual distance from the two ends was 6 cm, i.e., for f, the span was 138 cm). For Z9 to Z12, because of the small eccentric pressure, legs were not installed. For the second batch of test components (this batch of test components all were fitted with legs), the average value of $\Delta f_g/\Delta f$ was larger than the average value of f_g/f. This reflects the effect of the increase in stiffness of the leg section.

Figure 9 illustrates the whole procedure for calculating $\frac{1}{\rho}$ according to the method of computation suggested in reference (6) by dotted lines. The lines coincide fairly well.

IV. Results of Cracking Experiments and Analysis

Measurements of the cracks of the test components under large eccentric pressure or close to large eccentric pressure were taken (Z-1 and ZIV-1 were not measured). The measured results are shown in Table 4.

The calculations followed the original suggestion,[2] i.e., the average gap of the cracks were calculated according to the formula for structural components subjected to bending as suggested in the codes, ψ was according to equation (5). The stress of the steel reinforcement was calculated according to the following equation as originally suggested[2]:

$$\sigma_g = \frac{Ne_0\left[1.15 - (0.45 - 0.5n\mu)\frac{h_0}{e_0}\right]}{A_g h_0} \tag{10}$$

The applicable range of the above equation is $e_0/h_0 \geq 0.55$.

It can also be calcuated as a structural component subjected to bending by using the bending moment N_e and the steel reinforcement $A_g + \frac{N}{\sigma_g}$ as equivalent substitutions. (In eccentric pull, the "+" sign is changed to the "-" sign.) At this time,

$$\sigma_g = \frac{Ne}{A_g \eta h_0} - \frac{N}{A_g} \tag{11}$$

Table 4. Comparison of the Measured Values and Computed Values of Cracks

Test Components	d μ	l_f^s (cm)	l_f (cm)	l_f^s/l_f	Load (t)	Computed stress of steel reinforcement σ_g (kg/cm^2)	δ_f^s (mm)	δ_f (mm)	δ_f^s/δ_f	δ^s_{max} (mm)	$r' = \frac{\delta^s_{max}}{\delta_f^s}$	$r = \frac{\delta^s_{max}}{\delta_f}$
Z—2	173	10.95	11.45	0.955	8	4000	0.131	0.202	0.65	0.198	1.51	0.98
3	130.5	10.22	9.7	1.055	12	1940	0.0492	0.0755	0.653	0.088	1.79	1.16
4	131.5	9.86	9.74	1.015	18	2920	0.0845	0.1355	0.625	0.132	1.56	0.98
5	131	9.81	9.72	1.010	15	1780	0.0597	0.0687	0.87	0.099	1.66	1.44
					20	2370	0.0885	0.103	0.858	0.154	1.74	1.50
6	130.0	10.35	9.67	1.068	25	2950	0.0955	0.1373	0.695	0.132	1.38	0.96
7	106.3	9.4	8.68	1.082	30	1700	0.0373	0.0605	0.615	0.099	2.65	1.64
8	180	10.06	11.75	0.865	30	3170	0.1365	0.156	0.874	0.176	1.29	1.13
ZII—1	210	19.2	13.0	1.475	18	1840	0.0792	0.073	1.087	0.143	1.81	1.96
					22	2260	0.1242	0.1063	1.168	0.158	1.6	1.86
2	155	9.77	10.7	0.912	30	2000	0.0570	0.0767	0.742	0.077	1.35	1.01
					40	2660	0.0965	0.1172	0.823	0.143	1.48	1.22
ZV—1	209	10.3	12.98	0.740	28	1630	0.0636	0.070	0.911	0.11	1.73	1.57
2	151	9.77	10.52	0.928	35	2000	0.0632	0.0858	0.737	0.099	1.56	1.15
					45	2570	0.1090	0.1205	0.905	0.165	1.51	1.37
ZVII—2	151	14.1	10.52	1.338	20	1760	0.0577	0.0738	0.782	0.069	1.72	1.34
					27	2380	0.1165	0.1104	1.053	0.187	1.6	1.69
Average l_f^s/l_f =				1.036		Average δ_f^s/δ_f =			0.826		1.658	1.352
						Mean square error σ =			0.156			0.296
						Scattering percentage C_v =			0.189			0.219

For η, we can use the equation (4) suggested for structural components subjected to bending, but $n\mu$ should be equivalently substituted by $(n\mu)$,

$$(n\mu) = n \frac{A_g + \dfrac{N}{\sigma_g}}{bh_0} \tag{12}$$

then

$$\eta = 1 - 0.4\sqrt{(n\mu)} \tag{13}$$

Because the effect is not large, the effect of the pressured steel reinforcement is not taken into consideration in the computation.

Because η on the right side of equation (11) also contains σ_g, therefore test calculations must be performed, but it easily converges.

After comparison with equation (10), the differences of the two are usually within 10 percent. When the eccentricity is small, the percentage of fitted reinforcements is higher (generally belonging to damage by small eccentric pressure). Since the error of equation (10) is larger, it requires study and revision.

Figure 2 shows the computed σ_g for Z1 - Z4 in dotted lines. It can be seen that sometimes the computed values are much larger. This is related to the inherent error of the computational formula and also related to the fact that the points of measurement may not always be on the cracked section. But this type of deviation will gradually lessen as the load increases.

To be able to calculate test components with a relatively small eccentricity and more fitted reinforcements in the experiment, the computed values δ_f listed in Table 4 have all been obtained from σ_g determined uniformly according to equation (11).

Actually, when $e_0/h_0 < 0.55$, such as ZII-2 ($e_0/h_0 = 0.555$), and when $N = 40t$, i.e., when $N/N_p^s = 0.77$, $\delta_{f\,max}^s$ reaches only 0.143 mm; ZV-1 ($e_0/h_0 = 0.455$, $N/N_p^s = 0.842$, $\delta_{f\,max}^s = 0.11$ mm; ZV-2 ($e_0/h_0 = 0.51$), $N/N_p^s = 0.875$, $\delta_{f\,max}^s = 0.165$ mm. When considering an increase of 50 percent due to long term effect, the requirement of not surpassing 0.3 mm can still be satisfied. Therefore, according to the original suggestion, when $e_0/h < 0.55$, gererally the width of the cracks need not be checked,[2] and this may be feasible.

Table 4 shows the average $\delta_f^s/\delta_f = 0.826$, $\sigma = 0.156$, $C_v = 0.189$, coinciding better than the data on cracks checked for structural components subjected to bending in the past (For the latter,they are respectively 0.804, 0.2245, 0.279[5]); the average $\tau = 1.352$, $\sigma = 0.296$, $C_v = 0.219$, also having less dispersion than structural components subjected to bending (For the latter, they are respectively 1.405, 0.380 and 0.270).

Possibly the greatest width of cracking determined by statistical data (according to a definite percentage of assurance)[2]:

$$\delta_{f\,max} = (100 + 0.2\frac{d}{\mu})\ \frac{\sigma_g}{E_g},\ (\mathrm{mm}) \quad (14)$$

According to the data in Table 4, the percentage of assurance of equation (14) is 70.5 percent, coinciding with the statistics for structural components subjected to bending in reference (2). When the two sets of data of slightly higher loads are deleted, the percentage of assurance can reach 80 percent

V. Conclusion

Based on these experiments, we have formulated the following two preliminary views:

1. The experiments showed the computational formula for calculating stiffness under a load suggested in the past generally coincides better with the actual situation. But the suggestion of completing the simplified computations for the whole process should be followed and the effects of longitudinal bending of the long column should be studied.

2. Comparative computations showed the computation of the width of the cracks originally suggested still coincides with the actual situation. The formula for calculating the maximum width of the cracks based on the original suggestion and according to statistical determination still has a sufficient percentage of assurance for eccentrically pressured components.

In developing the test components, a lot of help was received from the Nanjing Concrete Components Plant. In preparing and carrying out the experiments and in testing and compiling reports, enthusiastic help was received from all the comrades of the structural laboratory and Comrade Yuan Biguo [5913 1801 2654] of the civil engineering construction teaching and research group. In the first draft of this article, the numbering of two beams was reversed. This was pointed out by Comrade Zhang Liren [1728 4539 0086] of the Second Engineering Department of the Hunan Provincial Coal Construction Company. We thank them all.

Because of limited space, the experimental results and analysis of crack resisting load and breaking load were not included in this article.

Because the number of experiments conducted was insufficient, analysis was not sufficiently carried out in depth. The information is provided only as reference. Criticism and correction of mistakes are welcomed.

REFERENCES

1. Fifth Department of the Nanjing Institute of Technology: Preliminary exploration of computing the stiffness of eccentrically pressured structural components of reinforced concrete (preliminary draft), 1977. 1.

2. Stiffness and crack scientific research group of the civilian engineering construction staff: Calculation of the deformation and crack of reinforced concrete structural components. NANJING GONGXUEYUAN XUEBAO [JOURNAL OF THE NANJING INSTITUTE OF TECHNOLOGY], 1977 single issue.

3. Stiffness and crack scientific research group of the civilian engineering construction staff: Calculation of the deformation and crack of reinforced concrete structural components. JOURNAL OF THE NANJING INSTITUTE OF TECHNOLOGY, No 2, 1978.

4. Fifth Department of the Nanjing Institute of Technology: Experimental research of the deformation and crack and shear strength of the reinforced concrete beam. JILIN JIANZU JIXHU TONGXUN [JILIN ARCHITECTURAL TECHNIQUES BULLETIN], 1976. 2.

5. Fifth Department of the Nanjing Institute of Technology: Calculation of the deformation and crack of structural components of reinforced concrete subjected to bending. "Selected research reports on reinforced concrete structures" Chinese Architectural Industry Press, 1977.

6. Ding Dajun [0002 1129 6874]: Preliminary suggestion on the whole procedure to compute the deflection of reinforced concrete structural components subjected to bending and large eccentric pressure, mimeographed book of the Nanjing Institute of Technology, 1979. 10.

9296
CSO: 8111/0598

TABLE OF CONTENTS OF 'QICHE GONGCHENG' NO 1, 1981

Beijing QICHE GONGCHENG [AUTOMOBILE ENGINEERING] in Chinese No 1, 1981 inside front cover

9717
CSO: 4008/296

TABLE OF CONTENTS OF 'WUSUN JIANCE' NO 1, 1981

Shanghai WUSUN JIANCE [NONDESTRUCTIVE TESTING] in Chinese No 1, 1981 preceding p 1

9717
CSO: 4008/294

TABLE OF CONTENTS OF 'JICHUANG YU YEYA' NO 1, 1981

Guangzhou JICHUANG YU YEYA [MACHINE TOOL AND HYDRAULICS] in Chinese No 1, 1981 inside front cover

9717
CSO: 4008/289

PUBLICATIONS

TABLE OF CONTENTS OF 'HAIYANG', DEC 1980

Beijing HAIYANG [OCEANS] in Chinese No 2, 15 Dec 80 p 32

6168
CSO: 4008/157

TABLE OF CONTENTS OF 'LIXUE XUEBAO' NO 2, 1981

Beijing LIXUE XUEBAO [ACTA MECHANICA SINICA] in Chinese No 2, 1981 inside back cover

9717
CSO: 4008/340

TABLE OF CONTENTS OF 'SHENGXUE XUEBAO' NO 2, 1981

Beijing SHENGXUE XUEBAO [ACTA ACUSTICA] in Chinese No 2, 1981 on back cover

9717
CSO: 4008/300

TABLE OF CONTENTS OF 'JIGUANG' VOL 8 NO 2, 1981

Shanghai JIGUANG [LASER JOURNAL] in Chinese Vol 8 No 2, 1981 inside back cover

9717
CSO: 4008/282

TABLE OF CONTENTS OF 'WULI' VOL 10 NO 2, 1981

Beijing WULI [PHYSICS] in Chinese Vol 10 No 2, 1981 on back cover

[Text] Knowledge and Progress

9717
CSO: 4008/286

TABLE OF CONTENTS OF 'YINGYONG SHUXUE XUEBAO' VOL 4 NO 1, 1981

Beijing YINGYONG SHUXUE XUEBAO [ACTA MATHEMATICAE APPLICATAE SINICA] in Chinese Vol 4 No 1, 1981 on back cover

Displacements of the Surface of an Elastic Half-space Under the Action of a Suddenly Applied Point Force......Wang Kecheng [3769 0668 2052], Hunan Institute of Computing Technology; Wang Yirun [3769 6318 5549], Hunan University (91)

9717
CSO: 4008/298

TABLE OF CONTENTS OF 'DICENGXUE ZAZHI' VOL 5 NO 1, 1981

Beijing DICENGXUE ZAZHI [JOURNAL OF STRATIGRAPHY] in Chinese Vol 5 No 1, 1981 inside back cover

9717
CSO: 4008/295

TABLE OF CONTENTS OF 'DAQI KEXUE' VOL 5 NO 1, 1981

Beijing DAQI KEXUE [SCIENTIA ATMOSPHERICA SINICA] in Chinese Vol 5 No 1, 1981
inside back cover

[Excerpt] Articles

8717
CSO: 4008/274

TABLE OF CONTENTS OF 'GAONENG WULI YU HE WULI' VOL 5 NO 2, 1981

Beijing GAONENG WULI YU HE WULI [PHYSICA ENERGIAE FORTIS ET PHYSICA NUCLEARIS] in Chinese Vol 5 No 2, 1981 inside back cover

9717
CSO: 4009/287

AUTHOR: DAI Hewu [2071 0735 2976]
CHEN Misheng [7115 4410 3932]
CHEN Wenmin [7115 2429 2404]

ORG: All of the Beijing Research Institute of Coal Chemistry (CMRI)

TITLE: "The Study of Distribution of Coal-bearing Substances of Different Ages and Coal Features in China"

SOURCE: Taiyuan RANLIAO HUAXUE XUEBAO [JOURNAL OF FUEL CHEMISTRY AND TECHNOLOGY] in Chinese Vol 9 No 1, Mar 81 pp 1-13

TEXT OF ENGLISH ABSTRACT: The distribution characteristics of coal-bearing accumulation at different coal ages in China were studied systematically in this paper. The distinctions of coal resources in some major accumulation stages and also the coal nature of different coal bearing systems and their patterns of changes were described. Apparent distinctions in distribution characteristics and their coal features at different geological ages were found.

AUTHOR: XU Xiao [1776 2556]
LI Taiqian [2621 3141 6197]
WEI Meizhong [7614 2734 0022]
ZHANG Jingcheng [1728 6975 3397]
XU Shuying [1776 3219 5391]
SHI Meiren [0670 5019 0088]
LI Boling [2621 2672 0109]

ORG: All of the Institute of Coal Chemistry, Chinese Academy of Sciences

TITLE: "Isolation of Isoprene from C_5 Fraction of Cracked Naphthas. Verification Experiment for Mathematical Modeling"

SOURCE: Taiyuan RANLIAO HUAXUE XUEBAO [JOURNAL OF FUEL CHEMISTRY AND TECHNOLOGY] in Chinese Vol 9 No 1, Mar 81 pp 14-28

TEXT OF ENGLISH ABSTRACT: To obtain high purity isoprene from C_5 fraction of cracked naphtha, extractive distillation and rectification were generally employed. Both of them could be described by mathematical modeling. In this paper, experimental data for verification of models were presented.

A ϕ32 mm column with 92 sieve plates was used and it was equipped with 9 sites along the column both for sampling and temperature measuring. The experiments were carried out in this column successively according to the sequence in the flow diagram, i.e., first extractive distilling column for separating C_5 alkanes and

[Continuation of RANLIAO HUAXUE XUEBAO Vol 9 No 1, Mar 81 pp 14-28]

alkenes from dienes, first rectifying column to remove the components heavier than isoprene, second extractive distilling column for separating other alkanes and cyclopentadiene from isoprene, and the last procedure, second rectifying column to remove the components lighter than isoprene. The C_5 fraction with 20 components from the cracking unit of a petrochemical plant was used as feed stock and DMF was used as the solvent.

The profiles of compositions of each component and temperatures along the column of the above-mentioned four procedures under their appropriate operating conditions at equilibrium were given. The corresponding analytical methods which involved about 10 chromatographic columns used independently or in combination were also presented.

9717
CSO: 4009/246

AUTHOR: LI Guohao [2621 0948 6275]
YI Jianguo [2496 1696 0948]
CHEN Zhongyan [7115 1813 1693]

ORG: None

TITLE: "Earthquake-Resistant Analysis of the Luan River Bridge. (2) Earthquake Response Analysis"

SOURCE: Shanghai TONGJI DAXUE XUEBAO [JOURNAL OF TONGJI UNIVERSITY] in Chinese No 1, 1981 pp 1-14

TEXT OF ENGLISH ABSTRACT: Based on a previous report on the field test of a highway continuous beam bridge, this paper presents the analysis of the earthquake response of the bridge.

In this paper, simplified mechanical models of the bridge are proposed based on the theoretical analysis of the field test results. The earthquake responses of the bridge are computed from the typical response spectrum and the earthquake acceleration waves inputted by using the DR analysis programs (Dynamic Response Analysis Programs for Plane Member Structure). Finally, the safety degree and measures of earthquake resistance are discussed through a comparison between the results gained from the strength checking computations of the dangerous sections of the piles of two different models.

AUTHOR: SUN Jun [1327 6874]
ZHANG Dexing [1728 1795 5281]
ZHANG Yusheng [1728 3768 3932]

ORG: None

TITLE: "Visco-elastic and Visco-plastic Analysis of Rock Stratum Around Deep-seated Tunnel Opening"

SOURCE: Shanghai TONGJI DAXUE XUEBAO [JOURNAL OF TONGJI UNIVERSITY] in Chinese No 1, 1981 pp 15-22

TEXT OF ENGLISH ABSTRACT: In this paper is proposed a rheological model with the Kelvin and Bingham bodies coupled in series, describing the instantaneous deformation and creep of a rock stratum which is assumed to be a uniform and homogeneous continuum, around a deep-seated tunnel opening, and for this purpose a finite element program for plane strain problems has been set up. The model with its computation program is suited for instantaneous elasticity, visco-elastic and visco-plastic behaviors of the rock around the tunnel opening, and is especially suited for studying the viscous behavior of soft rock, such as rock salt, shale, marl, etc. A numerical example is given to illustrate the use of the method.

AUTHOR: YAN Deyue [7346 1795 1471]
LI Guoying [2621 0948 3853]
JIANG Yuansheng [3068 0337 3932]

ORG: LI of Jiangsu Institute of Technology; JIANG of Jilin University

TITLE: "The Molecular Weight Distribution of Multi-functional Living Polymers"

SOURCE: Shanghai TONGJI DAXUE XUEBAO [JOURNAL OF TONGJI UNIVERSITY] in Chinese No 1, 1981 pp 23-42

TEXT OF ENGLISH ABSTRACT: In this paper, the general expressions of molecular weight distribution function and average degree of polymerization of multi-functional living polymer with arbitrary functionality are derived by means of deliberately solving the set of kinetic differential equations. For the double cruciform, star-shaped and comb-shaped living polymers, the branched chain length distribution and the average number of branched chains are also treated. As special examples, some of the practical cases are discussed in which the living polymers were respectively generated by mono-functional, bifunctional or trifunctional initiators. The formulas concerning linear polymers are compared with those reported in the past.

AUTHOR: CHEN Yangji [7115 2254 7535]
XU Yunyuan [1776 6663 3293]

ORG: None

TITLE: "Approximate Method for Determining the Temperature Stresses in Space Latticed Trusses"

SOURCE: Shanghai TONGJI DAXUE XUEBAO [JOURNAL OF TONGJI UNIVERSITY] in Chinese No 1, 1981 pp 43-56

TEXT OF ENGLISH ABSTRACT: This paper presents an approximate method for calculating the stresses in space latticed trusses due to temperature changes. The results are compared with those obtained by precise solutions with a digital computer, and the discrepancies are found to be within allowable limits. In addition, the conditions under which the temperature stresses may be neglected are also given.

AUTHOR: TU Xiangyuan [1458 0686 6678]
SHEN Rongfang [3088 2837 5364]
HE Jianli [0149 0256 7787]

ORG: None

TITLE: "Study of Wind Load Problems"

SOURCE: Shanghai TONGJI DAXUE XUEBAO [JOURNAL OF TONGJI UNIVERSITY] in Chinese No 1, 1981 pp 57-67

TEXT OF ENGLISH ABSTRACT: This paper discusses the various problems of characteristics of daily wind, yearly wind, the wind during using period, and the frequencies and time intervals of strong wind. The respective statistical parameters and distribution regularities are obtained. Meteorological data were taken from 30 meteorological stations located throughout the PRC.

Based on the above discussion, the paper also presents the suggestion of methods for wind analysis to be used in the Wind Load Code of China.

AUTHOR: YAO Zukang [1202 4371 1660]
HUAN Layuan [2719 5198 0337]
LENG Peiyi [0397 1014 5030]
et al.

ORG: None

TITLE: "Loading Tests of Concrete Pavements on Elastic Foundation"

SOURCE: Shanghai TONGJI DAXUE XUEBAO [JOURNAL OF TONGJI UNIVERSITY] in Chinese No 1, 1981 pp 68-77

TEXT OF ENGLISH ABSTRACT: It has been shown by loading tests on concrete slabs that the analytical results of deflections and strains of slabs resting on elastic semi-infinite continuum by the finite element method coincide well with the measured values when the loads are applied on the interior or edge-center of the slabs. However, the resilient modulus of the foundation under the slab by interior loading should be two to three times greater than that from the bearing plate test. As for corner loading, the Winkler foundation model is preferable.

AUTHOR: YANG Yanxiong [2799 1693 3574]
GU Yuping [7357 5148 1627]

ORG: None

TITLE: "The Measurement of Hardening Index n' for Metals and Its Application in Fracture Mechanics"

SOURCE: Shanghai TONGJI DAXUE XUEBAO [JOURNAL OF TONGJI UNIVERSITY] in Chinese No 1, 1981 pp 78-83

TEXT OF ENGLISH ABSTRACT: This paper represents an effective testing technique for the measurement of hardening index n' of metals. Also, the significance of the hardening index and its application in fracture mechanics is mentioned. A method of converting the J_{1c} value into the K_{1c} value by the J_{1c} and COD measurements using small specimens is described in this paper.

AUTHOR: SHI Junliang [2457 0193 5328]
HU Yunkang [5170 6663 1660]
SONG Ziyan [1345 1311 1750]

ORG: None

TITLE: "Selecting Calculation of Three-port Modulating Valve in Cooling System with Surface Cooler"

SOURCE: Shanghai TONGJI DAXUE XUEBAO [JOURNAL OF TONGJI UNIVERSITY] in Chinese No 1, 1981 pp 84-94

TEXT OF ENGLISH ABSTRACT: This paper solves the selecting calculation of a three-port valve with a theoretical method and gives the equations for computing the static characteristics of surface cooler, the pulsation of total flow of the valve, and the actual adjustable range of the valve. By means of an engineering system which has operated normally for many years, the above theoretical method is verified.

AUTHOR: MA Zhichao [7456 1807 6389]

ORG: None

TITLE: "The Construction of Perspectives by means of Planes Parallel to the Picture Plane instead of Using the Vanishing Point"

SOURCE: Shanghai TONGJI DAXUE XUEBAO [JOURNAL OF TONGJI UNIVERSITY] in Chinese No 1, 1981 pp 95-107

TEXT OF ENGLISH ABSTRACT: The perspective direction of a desired line is usually determined by connecting a given point to the vanishing point of this line. If the perspective of another point in the desired line which lies in a plane parallel to the picture is found, the perspective direction of the desired line can be determined without referring to the vanishing point. This paper, based on expounding on this construction, sums up and presents the graphical conditions, the basic graphics in various cases and the auxiliary graphics using planes parallel to the picture plane instead of the vanishing point.

AUTHOR: PAN Hongxuan [3382 1363 5503]

ORG: None

TITLE: "Examination of the Lanjin and Jihong Bridges in Yunnan"

SOURCE: Shanghai TONGJI DAXUE XUEBAO [JOURNAL OF TONGJI UNIVERSITY] in Chinese No 1, 1981 pp 108-116

TEXT OF ENGLISH ABSTRACT: Lanjin Bridge at Jingdong and Jihong Bridge at Yongping were ancient suspension bridges over the Lancang River made of iron chains. According to historical records, the Lanjin Bridge was built in the period of the Emperor Ming of the Eastern Han Dynasty. It was a famous ancient bridge widely known throughout the world, and was mentioned frequently by scholars of technical history in their theses. Now, through field investigation and the study of all available literature, it is found that the Lanjin Bridge no longer exists. The site of the Jihong Bridge at Yongping was a ferry before and during the Western Han. That bridge was constructed not later than the time of the "Three Kingdoms." By the time of Chenghua of the Ming Dynasty, that bridge was reconstructed to a suspension bridge made of iron chains, and is now the most ancient suspension bridge in China. When the Yongcheng prefecture was set up by the 12th year of Emperor Ming of the Eastern Han Dynasty, Jihong Ferry or Bridge became an important traffic junction, joining all the counties in that prefecture. Therefore, the Lanjin Bridge on record is possible the Jihong Bridge.

9717
CSO: 4009/222

END

END OF
FICHE
DATE FILMED